Human Molecular Genetics, 2008, Vol. 17, No. 1 **52–70**
doi:10.1093/hmg/ddm284
Advance Access published on October 2, 2007

Protein phosphatase 1 binds to the RNA recognition motif of several splicing factors and regulates alternative pre-mRNA processing

Tatyana Novoyatleva[1], Bettina Heinrich[1], Yesheng Tang[1], Natalya Benderska[1], Matthew E.R. Butchbach[4], Christian L. Lorson[5], Monique A. Lorson[5], Claudia Ben-Dov[2], Pascale Fehlbaum[3], Laurent Bracco[3], Arthur H.M. Burghes[4], Mathieu Bollen[6] and Stefan Stamm[1,7]*

[1]University of Erlangen, Institute for Biochemistry, Fahrstraße 17, Erlangen 91054, Germany, [2]ICREA and Centre de Regulacio Genomica, Passeig Maritim 37–49, Barcelona 08003, Spain, [3]Exonhit, ExonHit Therapeutics, 65 Boulevard Massena, Paris 75013, France, [4]Department of Molecular and Cellular Biochemistry, Ohio State University, 363 Hamilton Hall, 1645 Neil Avenue, Columbus, OH 43210-1218, USA, [5]Life Sciences Center, Department of Veterinary Pathobiology, University of Missouri, 471G, 1201 Rollins Road, Columbia, MO 65211-7310, USA, [6]Laboratory of Biosignaling and Therapeutics, Department of Molecular Cell Biology, Faculty of Medicine, KULeuven, Belgium and [7]Department of Molecular and Cellular Biochemistry, 741 South Limestone, BBSRB, Lexington, KY 40536

Received June 25, 2007; Revised and Accepted September 27, 2007

Alternative splicing emerges as one of the most important mechanisms to generate transcript diversity. It is regulated by the formation of protein complexes on pre-mRNA. We demonstrate that protein phosphatase 1 (PP1) binds to the splicing factor transformer2-beta1 (tra2-beta1) via a phylogenetically conserved RVDF sequence located on the RNA recognition motif (RRM) of tra2-beta1. PP1 binds directly to tra2-beta1 and dephosphorylates it, which regulates the interaction between tra2-beta1 and other proteins. Eight other proteins, including SF2/ASF and SRp30c, contain an evolutionary conserved PP1 docking motif in the beta-4 strand of their RRMs indicating that binding to PP1 is a new function of some RRMs. Reducing PP1 activity promotes usage of numerous alternative exons, demonstrating a role of PP1 activity in splice site selection. PP1 inhibition promotes inclusion of the survival of motoneuron 2 exon 7 in a mouse model expressing the human gene. This suggests that reducing PP1 activity could be a new therapeutic principle to treat spinal muscular atrophy and other diseases caused by missplicing events. Our data indicate that the binding of PP1 to evolutionary conserved motifs in several RRMs is the link between known signal transduction pathways regulating PP1 activity and pre-mRNA processing.

INTRODUCTION

The recent sequencing of metazoan genomes demonstrated the importance of alternative splicing as a major mechanism for generating multiple gene products from the unexpected low number of genes. The vast majority of human protein-encoding genes undergo alternative splicing (1,2). Unlike promoter activity that predominantly regulates the abundance of transcripts, alternative splicing influences the sequence of the mRNAs and their encoded proteins. As a result, it influences binding properties, intracellular localization, enzymatic activity, protein stability and post-translational modification of numerous gene products. The biological effects evoked by alternative splicing are diverse and range from a complete loss of function to subtle effects (3). Since splice sites are highly degenerate, protein complexes forming on the pre-mRNA help in the high-fidelity recognition of exons. SR-proteins and hnRNPs are the major classes of proteins identified in these complexes. They generally possess RNA-binding and protein-interaction domains that allow weak, transient binding between protein and pre-mRNA as well as between proteins. The combination of these multiple weak

*To whom correspondence should be addressed. Tel: +49 91318524622/8593230896; Fax: +49 91318524605/8593231037; Email: stefan@stamms-lab.net

interactions ultimately leads to the proper recognition of exons by the spliceosome (4,5).

Transformer2-beta1 (tra2-beta1) is one of the proteins that regulate splice site selection by recruiting regulatory proteins to exon sequences. It is an SR-like protein and is composed of two RS-domains flanking a central RNA-recognition motif. The RS-domains allow interaction between tra2-beta1 and other SR-proteins, as well as homomultimerization (6–8). Tra2-beta1 binds to a degenerate RNA sequence that is rich in purine residues and is more frequently found in exons than in introns, which suggests that its major function is the identification of exonic sequences on pre-mRNA. The protein promotes in a concentration-dependent manner the inclusion of a large number of alternative exons that contain its recognition sequence (9,10). It was first identified in Drosophila, where it is part of a cascade of alternative splicing decisions that ultimately determine the sex of the flies (11,12). Like other SR-proteins, tra2-beta1 is predominantly nuclear where it is localized in a characteristic speckled pattern. Its pre-mRNA undergoes alternative splicing, giving rise to at least five mRNA isoforms that are subject to autoregulation, which allows the precise control of the cellular tra2-beta1 concentration (10). Despite this autoregulation, tra2-beta1 expression is unphysiologically high in breast and ovarian cancer (13,14), hypoxia (15,16), silicosis (17) and arteriosclerosis (18). Similar to many other mRNAs generated by alternative splicing, the formation of tra2-beta isoforms is subject to developmental and cell-type specific control (7), which changes in response to cellular stimulation. For example, neuronal activity shifts the isoform ratios of tra2-beta toward the brain and testis-specific isoform tra2-beta3 (19). Such signal-dependent changes of alternative splicing are frequently observed (20,21). The underlying mechanism causing a rapid switch between alternative mRNA isoforms is unknown, but since it does not require protein-synthesis in most cases, it is most likely due to changes in reversible protein phosphorylation (20,22).

SR-proteins are phosphorylated by several kinases, including the Clk/Sty kinase family (cdc2-like kinases, Clk1-4), the SRPK family (SRPK1,2), mammalian PRP4, topoisomerase I and CDC2 kinase 2 (23). Functionally, phosphorylation of SF2/ASF regulates its interaction with the U170K protein, SRp40 and its homomultimerization. It can either increase protein : protein interaction, e.g. between SF2/ASF and U170K or decrease protein : protein interaction, e.g. between SF2/ASF and SRp40 or tra2-alpha (24,25). As a result, a change in phosphorylation of SR-proteins influences their activity in splice site selection and can modulate alternative exon usage (22,26–28). Phosphorylation can either increase or decrease alternative exon usage, which most likely reflects that it can both promote and inhibit protein : protein interactions. Protein phosphatases cause the dephosphorylation of SR-proteins that is necessary for the transesterification reaction (29). Protein phosphatase 1 (PP1) (30) and protein phosphatase 2Cgamma (31) associate with complexes formed on pre-mRNA and can be identified in the B complex (32). PP1 or PP2A-mediated dephosphorylation are involved in the structural rearrangements that are necessary for the transition from the first to second step of splicing (33). However, the binding partners and dephosphorylation targets of the phosphatases in the spliceosome are unknown.

The physiological importance of the correct splice site selection is most obvious in human diseases caused by aberrant splicing. It has been estimated that up to 15% of diseases caused by mutations are due to changes in splice site selection (34–36). One of these diseases is spinal muscular atrophy (SMA). SMA is caused by the loss of the SMN1 gene, which encodes the survival of motoneuron (SMN) protein that is ubiquitously expressed and necessary for motoneuron survival. In addition to SMN1, humans possess SMN2, an almost identical gene. However, the SMN2 gene cannot compensate for the loss of SMN1, because it is differently spliced (37). Although the gene structure and mRNA sequences between SMN1 and SMN2 are almost identical, there is a single C→T exchange at position +6 in exon 7. Due to this difference, exon 7 is constitutively used in SMN1, but predominantly excluded in SMN2. The exclusion of exon 7 causes the production of an unstable protein with an altered C-terminus. Therefore, cells lacking both copies of SMN1 produce insufficient amounts of SMN protein, which leads to the death of motoneurons. Since promotion of SMN2 exon 7 usage could potentially cure the disease, its regulation was intensively studied. SMN1 exon 7 inclusion is dependent on a central, tra2-beta1-dependent exonic enhancer (37,38) and an SF2/ASF-dependent enhancer located on the 5′ part of the exon that is absent in SMN2 due to the C→T change (39). Since the tra2-beta1-dependent enhancer is still present in SMN2 exon 7, increasing the concentration of tra2-beta1 promotes its inclusion.

Here we show that tra2-beta1 contains an evolutionary conserved PP1-binding motif. This binding motif is located in the beta-4 strand of the RNA recognition motif (RRM). The sequence of the PP1-binding motif is also conserved in the beta-4 strand of eight other RRMs, including those of SF2/ASF, SRp30c and PTB (polypyrimidine tract-binding protein). PP1 binds to tra2-beta1 and dephosphorylates it, which modulates the interaction between tra2-beta1 and other SR proteins. PP1 inhibition promotes inclusion of SMN2 exon 7 in patient-derived cells and mouse models, suggesting that this might be a new strategy for the treatment of SMA.

RESULTS

Tra2-beta1 contains an evolutionary conserved, previously unrecognized motif in the beta-4 strand of its RNA recognition motif that binds to PP1

Tra2-beta1 is an SR-like protein. It was detected in all metazoans, except plants. The protein contains a central RRM flanked by two serine-arginine-(SR)-rich domains. We compared all known tra2-beta1 protein sequences and identified a conserved RVDF sequence downstream of the alpha 2 helix of the RRM (Fig. 1A). Comparison with solved RRM structures and the NMR structure of the tra2-beta1 RRM (protein database code: 2CQC) shows that this motif is located in the beta-4 strand of the RRM. The motif corresponds to the consensus RVDF sequence that is present in most binding partners of PP1. This docking motif interacts with a hydrophobic

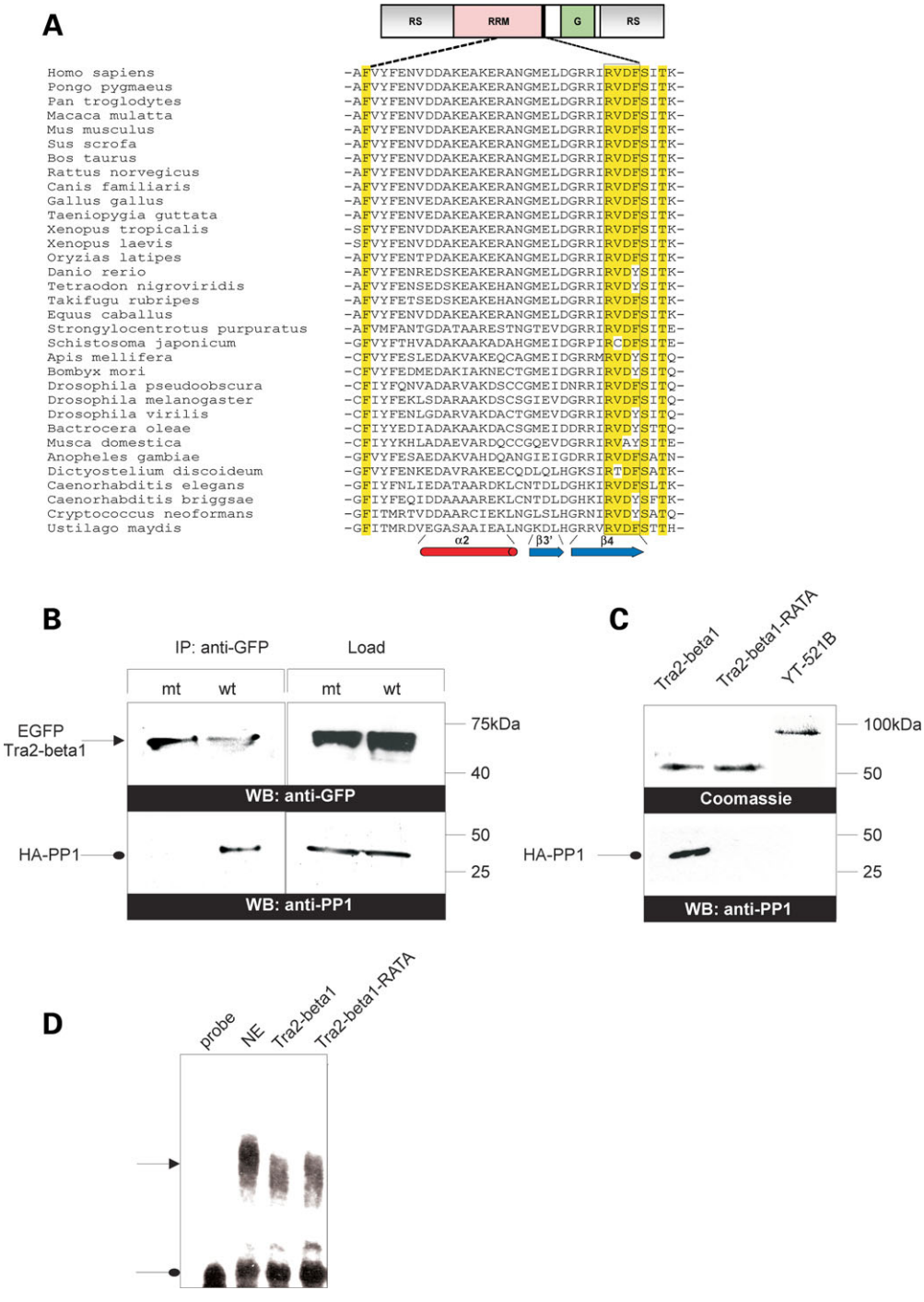

Figure 1. PP1 binds to a conserved motif in tra2-beta1 – (**A**) Alignment of tra2-beta1 sequences from different species: The cartoon on the top shows the domain structure of tra2-beta1 (6), RS, arginine-serine-rich domain; RRM, RNA recognition motif; G, glycine-rich region. The black line shows the conserved RVDF motif. The alpha 2 helix and the downstream predicted beta-sheets based on the NMR-solution structure (PBD code: 2CQC) are indicated below. β3′ refers to a short beta strand that is sometimes present in loop 5 of the RRM (68). All available sequences corresponding to human tra2-beta1 residues 161–196 are aligned. A box indicates the RVDF motif implicated in PP1 binding. Residues that are conserved in all species are marked in yellow. (**B**) Coimmunoprecipitation of tra2-beta1 and PP1: EGFP-tra2-beta1 wild-type (wt), EGFP-tra2-beta1 with a RVDF to RATA mutation (mt) and HA-PP1cgamma were expressed in HEK293 cells. Protein complexes were precipitated with anti-GFP antisera and identified by subsequent western blot analysis with anti-GFP and anti-PP1. Pointed arrows indicate tra2-beta1 protein, round arrows indicate PP1 protein. About 10% of the proteins for immunprecipitations were loaded in the load control on the right. (**C**) Direct interaction between tra2-beta1 and PP1 proteins: Recombinant His-tagged tra2-beta1, His-tra2-beta1-RATA and His-YT521-B were immobilized on Ni^{2+}-agarose and incubated with recombinant PP1. After washing, proteins were detected by coomassie staining on PAGE gels and by western blot. YT521-B is a non-related protein serving as a negative control. (**D**) Gel retardation assay: 1 μg of nuclear extract (NE), recombinant tra2-beta1 and tra2-beta1-RATA were incubated with a purine-rich RNA probe and analyzed by native gel electrophoresis. The pointed arrow indicates the RNA : protein complexes, the round arrow the free probe.

channel of PP1 that is remote from the catalytic site (40,41). As in other PP1 interactors, the RVDF motif of tra2-beta1 is N-terminally flanked by basic residues at position −2 and/or −3 that promote the initial binding to PP1 (42). The RVDF is followed by three evolutionary highly conserved amino acids: S/non-polar/T. It is fully conserved in all tra2-beta1 sequences from vertebrates, except some fish species and non-vertebrate species, where it is changed to RVDY. However, a tyrosine at the last position is present in other PP1 interactors (43).

Since the sequence alignment suggests that there is a phylogenetically conserved PP1-binding site in tra2-beta1 sequences, we performed immunoprecipitations to test whether PP1 binds to tra2-beta1. As a negative control, we mutated the RVDF motif to RATA, which is known to destroy the ability of this sequence to bind PP1 (44). PP1 coimmunoprecipitates with tra2-beta1, indicating that both proteins can form a molecular complex. In contrast, no interaction between tra2-beta1-RATA and PP1 is observed (Fig. 1B). To rule out nucleic acid-mediated effects, benzonase was added to all immunoprecipitates. Even in the absence of benzonase, the interaction between PP1 and tra2-beta1 depended on the RVXF motif (Supplementary Material, Fig. S1A). To determine whether their interaction is direct, we analyzed the binding of purified recombinant proteins. Tra2-beta1 was generated using the baculovirus expression system as a His-tagged protein. After purification, tra2-beta1 was immobilized on Ni^{2+}-agarose and used as an affinity matrix for the binding of purified PP1. As shown in Figure 1C, PP1 bound to tra2-beta1, but not to tra2-beta1-RATA and not to the unrelated splicing factor YT521-B (45), demonstrating a direct protein : protein interaction between tra2-beta1 and PP1. To test whether mutating the RVDF motif into RATA disrupts the RRM, we performed gel retardation assays using recombinant proteins and a purine-rich synthetic RNA. As shown in Figure 1D, both proteins bound to the RNA, demonstrating that the mutation did not disrupt the overall structure of the RRM. Together, these data show that tra2-beta1 binds directly to PP1 via its conserved RVDF motif.

The RVDF motif promotes the colocalization between tra2-beta1 and PP1

Next, we investigated whether the colocalization between tra2-beta1 and PP1 depends on the RVDF motif. Both proteins exhibit a dynamic localization in the cell. Tra2-beta1 is mainly localized in nuclear speckles, but shuttles between nucleoplasma and cytosol where it accumulates under stress conditions, such as hypoxia (10,16). Mammalian cells express three highly related alpha, beta and gamma PP1 isoforms that are encoded by different genes. All isoforms exhibit a dynamic localization and depending on their interaction partners can be found in all cellular compartments (46). We concentrated on PP1gamma that is mostly localized throughout the cell but enriched in the nucleoli in cultured cells (47,48). In contrast, in neurons it is found in the soma, dendrites and presynaptic buttons (49,50). Since tra2-beta1 and PP1gamma exhibit a dynamic localization in the cell, we used mutants in a cotransfection assay to determine whether they colocalize *in vivo*. We forced tra2-beta1 protein into the cytosol by introducing a REV nuclear export signal (tra2-beta1-NES). We then determined whether PP1 would influence this altered cellular localization by comparing the tra2-beta1-RATA mutant that does not bind PP1 with the wild-type. Figure 2A–E shows the staining pattern that is obtained when expression constructs for each mutant are transfected separately. Tra2-beta1 and tra2-beta1-RATA are localized in the nucleoplasm and are enriched in a speckled structure. As expected, tra2-beta1-NES and tra2-beta1-RATA-NES are found in the cytosol, where the tra2-beta1-RATA-NES protein accumulates in cytosolic bodies. PP1 is found throughout the cell, but predominantly localized in the nucleoli. Next, we co-expressed EGFP-tagged tra2-beta1 with CFP-tagged PP1cgamma. We performed confocal microscopy to determine the colocalization of the proteins and found ∼30% of the fluorescence signal from the two proteins to be present in the same space (Fig. 2F–H, R). When we employed the tra2-beta1-RATA mutant that does not bind to PP1, this colocalization was reduced to less then 10% (Fig. 2J, K and R). We then tested whether PP1 would interfere with the cytosolic localization of the tra2-beta1 mutant containing a NES. Surprisingly, the EGFP-tra2-beta1-NES signal was no longer detected in the cytosol when CFP-PP1cgamma was coexpressed with it. In almost all cells, the proteins showed strong colocalization in the nucleus (Fig. 2L–N and R), indicating that the binding to PP1 is strong enough to antagonize the REV-NES. To again test the dependency on the RVDF motif, we coexpressed an EGFP-tra2-beta1-RATA-NES mutant with CFP-PP1cgamma. Now, PP1 is predominantly located in the nucleus and EGFP-tra2-beta1-RATA-NES is located in the cytosol. Under these conditions the colocalization was reduced from about 70–30% (Fig. 2O–R). Western blot analysis showed that all mutant proteins in this transfection assay were expressed at approximately the same level (Fig. 2S). It was unexpected that the introduction of a NES caused a stronger colocalization between tra2-beta1 mutants and PP1gamma. This could indicate that continuous shuttling and possibly subsequent nuclear and cytosolic phosphorylation–dephosphorylation events are necessary for a correct association with PP1. Together, the data show that although both proteins have a dynamic localization, they partially colocalize in cells. The quantification (Fig. 2R) shows that this colocalization depends on the presence of the PP1-binding motif.

PP1 dephosphorylates tra2-beta1 *in vitro* and *in vivo*

Next, we asked whether PP1 could dephosphorylate tra2-beta1. First, we investigated the effect of PP1 purified from rabbit skeletal muscle on recombinant tra2-beta1. Recombinant tra2-beta1 was phosphorylated *in vitro* by incubation with nuclear extract and ^{32}P-gamma ATP. The nuclear extract contains Clk/Sty kinases that phosphorylate SR-proteins (51), which can be detected by autoradiography of the labeled protein. We observed that comparable amounts of tra2-beta1-RATA showed stronger labeling with ^{32}P after incubation in nuclear extract, which probably indicated a lower phosphatase activity on the protein (Fig. 3A, lanes 3 and 4). To test whether phosphatase activities

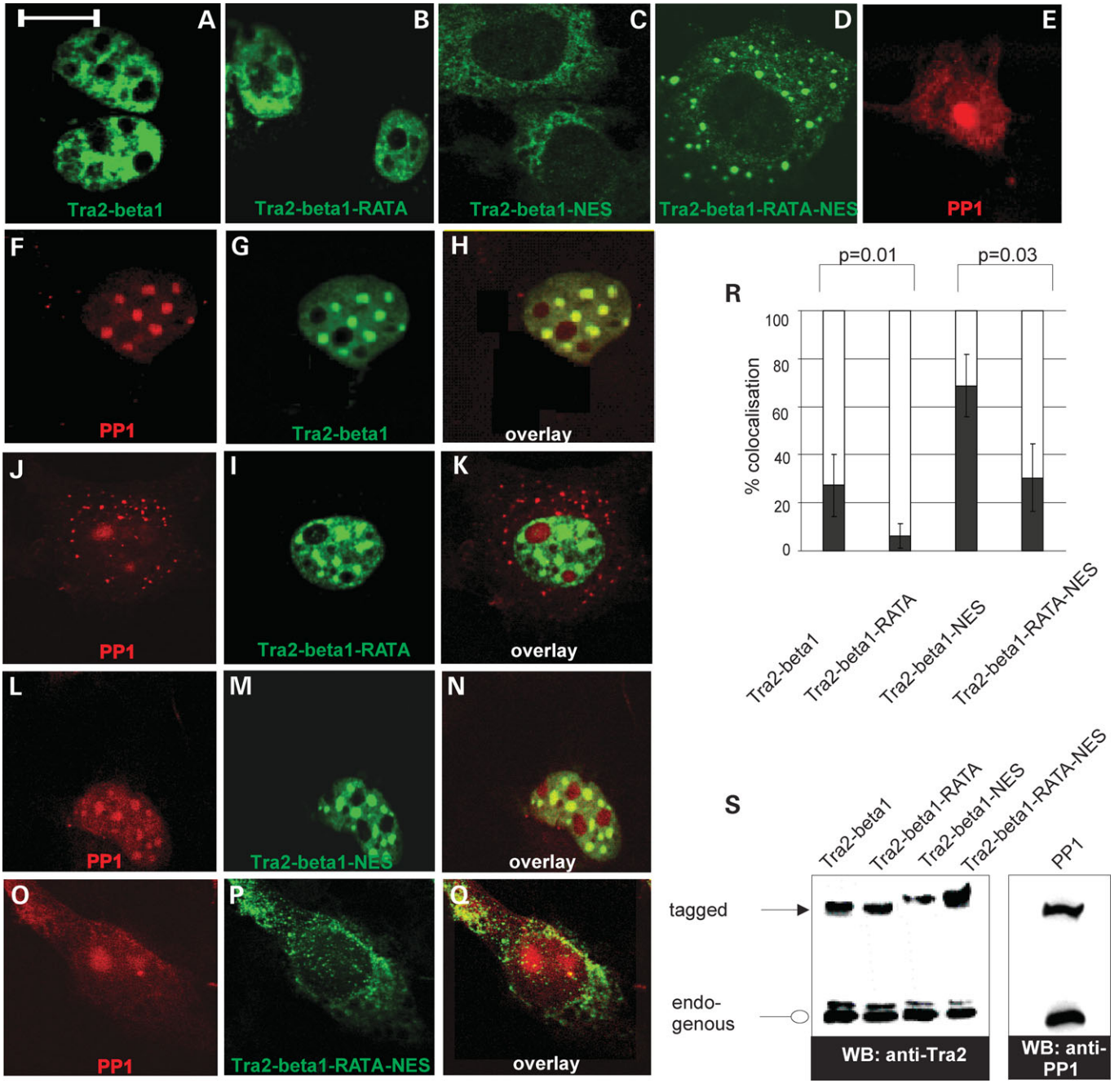

Figure 2. Colocalization between tra2-beta1 and PP1 – EGFP-tagged tra2-beta1 (green) and CFP-PP1cgamma (red) constructs were expressed in Cos 7 cells. Panels **A**–**Q** show representative cells. (A–E) Staining pattern obtained with individual proteins. (A) Tra2-beta1 wild-type, (B) tra2-beta1 lacking the PP1-binding site, (C) tra2-beta1 with a nuclear export signal (NES), (D), tra2-beta1 lacking the PP1-binding site and containing the NES and (E) CFP-PP1cgamma, (F–H) coexpression of tra2-beta1 and PP1, (J–K) coexpression of tra2-beta1-RATA and PP1, (L–N) coexpression of tra2-beta1-NES and PP1, (O–Q) coexpression of tra2-beta1-RATA-NES and PP1cgamma, (**R**) evaluation of the colocalization of at least 200 cells. Errror bars indicate the standard deviation; *P*-values of the student's test are indicated, (**S**) western blots showing the expression of the EGFP-tagged tra2-beta1 mutants and CFP-tagged PP1gamma. Cell lysates were analyzed by western blot using antisera against tra2-beta1 and PP1. An identical figure where PP1cgamma is shown in blue is given in Supplementary Material, Figure S5.

present in the nuclear extract could cause dephosphorylation, we monitored the labeling of tra2-beta1 without washing steps and did not observe a decrease in labeling after 1 h (Fig. 3A, lane 5). After removing the nuclear extract and performing stringent wash steps, the phosphorylated tra2-beta1 was incubated with PP1 and we found that PP1 action removed the ^{32}P-labeling of tra2-beta1. As a control, we used recombinant tra2-beta1-RATA. However, incubation of the purified protein with recombinant PP1 removed the ^{32}P labeling (data not shown), although there is no detectable

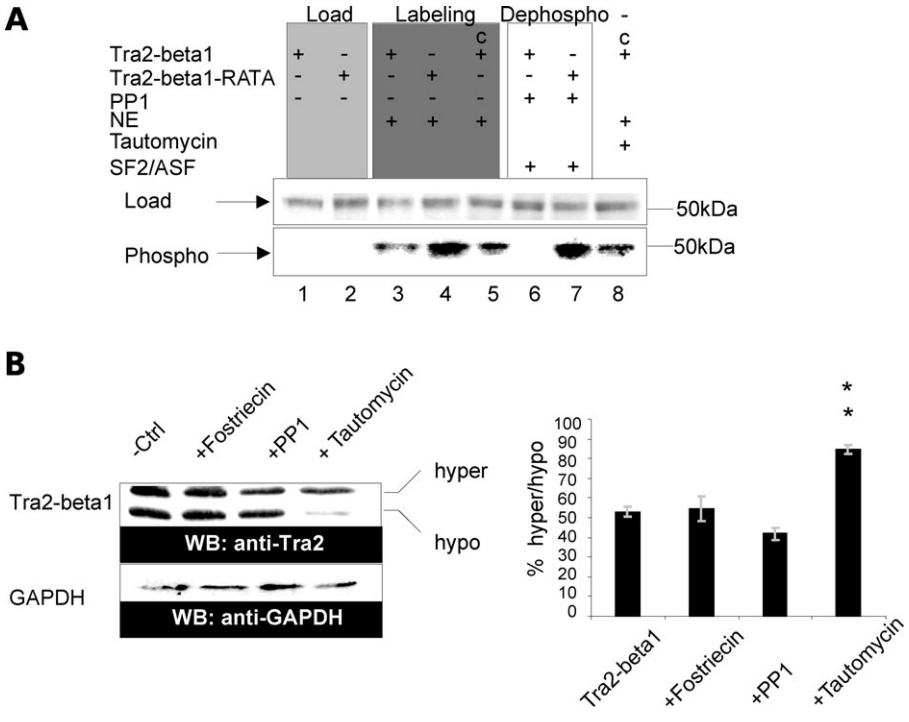

Figure 3. PP1 dephosphorylates tra2-beta1 – (**A**) Dephosphorylation *in vitro*: Recombinant His-tra2-beta1 was immobilized on Ni^{2+}-agarose and incubated with nuclear extract in the presence of ^{32}P-gamma ATP. The nuclear extract was then removed by stringent washing and purified ^{32}P-labeled tra2-beta1 was incubated with PP1. Tra2-beta1 was detected by coomassie staining (top row, load). The incorporation of ^{32}P was detected by phospho-imaging (lower row, phospho). The experimental conditions are listed on the top, NE: nuclear extract. The 'c' in lanes 5 and 8 indicates that nuclear extract used for labeling was not removed by washing. (**B**) Change of tra2-beta1 hyperphosphorylation *in vivo*: HEK293 cells were treated with fostriecin or tautomycin overnight, or a PP1c expression clone was transfected into the cells. The mobility of tra2-beta1 was determined by western blot using tra2-beta1 antisera and 15% PAGE gels (19). The graph shows the quantification of five independent experiments demonstrating a statistical significant difference (P=0.013, indicated by two stars) between tautomycin treatment and the other conditions. GAPDH was used as a loading control.

binding between the proteins in pull-down assays (Fig. 1C). Similar dephosphorylation without strong binding is frequently observed with PP1 acting on purified proteins and was used for activity assays (52). We therefore performed a competition assay and repeated the dephosphorylation in the presence of recombinant SF2/ASF that can bind to PP1 (see below, Fig. 6C). SF2/ASF was used in equimolar amounts to tra2-beta1 and tra2-beta1-RATA. In the presence of this competitor, tra2-beta1 is dephosphorylated by PP1, whereas tra2-beta1-RATA remains labeled with ^{32}P (Fig. 3A, lanes 6 and 7). Finally, adding the PP1 inhibitor tautomycin (53) to the phosphorylation reaction did not show any inhibition, indicating that tautomycin does not block the relevant kinase (Fig. 3A, lane 8). In addition, recombinant PP2A did not dephosphorylate tra2-beta1 (Supplementary Material, Fig. S2A). Together with the binding data demonstrating an interaction between the recombinant proteins, these data show that PP1 directly dephosphorylated tra2-beta1, which depends on the presence of the RVDF motif.

Next, we determined whether PP1 dephoshorylated tra2-beta1 *in vivo*. We analyzed the phosphorylation-dependent mobility of tra2-beta1 on high concentration PAGE gels. Similar to other SR-proteins, tra2-beta1 migrates as a hyper and hypophosphorylated form that can be detected after cells are immediately lysed in sample buffer containing 10% SDS, which blocks cellular phosphatases (19). The activity of PP1 in HEK293 cells was blocked by tautomycin, a cell permeable phosphatase inhibitor that blocks PP1 about four times more potently than protein phosphatase 2A (PP2A) and 10 000-fold more potently than protein phosphatase 2B (53). As shown in Figure 3B, treatment of cells with tautomycin caused a significant increase in the hyperphosphorylated form of tra2-beta1. To test whether tautomycin acts via PP2A, we blocked PP2A with its specific inhibitor fostriecin and did not observe a change between hyper and hypophosphorylated isoforms. Transfection of PP1c expression clones caused a small decrease of the hyperphosphorylated form. Together, these data show that PP1 can dephosphorylate tra2-beta1 both *in vivo* and *in vitro*.

Protein interactions of tra2-beta1 are controlled by PP1-mediated dephosphorylation

The work on SR-protein kinases demonstrated that an increase in phosphorylation influences protein : protein interaction of SR-proteins (24). We therefore investigated whether dephosphorylation regulates the interaction between tra2-beta1 and other proteins. Tra2-beta1 forms homodimers and can also heterodimerize with other SR-proteins, such as SF2/ASF (6,7). We thus asked whether the dimerization is influenced by PP1 action. We expressed EGFP-tagged wild-type tra2-beta1 and tra2-beta1-RATA in HEK293 cells. The

immunoprecipitates were analyzed with an antiserum specific for tra2-beta1, allowing the detection of endogenous protein (10). We found that in contrast to wild-type tra2-beta1, the tra2-beta1-RATA mutant no longer homomultimerizes with the endogenous tra2-beta1 (Fig. 4A). We then determined whether the known interaction between tra2-beta1 and SF2/ASF (7) is dependent on the PP1-binding site of tra2-beta1. Again, we immunoprecipitated tra2-beta1-RATA and wild-type tra2-beta1 with anti-GFP and detected SF2/ASF present in the immunoprecipitates by western blot. As shown in Figure 4B, no multimerization between SF2/ASF and tra2-beta1-RATA could be observed. All immunoprecipitations were performed in the presence of benzonase to omit RNA-mediated interactions. When these experiments were repeated without benzonase, interaction between the tra2-beta1-RATA mutant and other RNA-binding proteins could be detected, suggesting that both wild-type and mutant protein can assemble on the same RNA (Supplementary Material, Fig. S1B and C). Finally, we analyzed the phosphorylation-dependency of the binding between SF2/ASF and tra2-beta1 using recombinant proteins. As described earlier (Fig. 3A), baculovirus generated His-tra2-beta1 was phosphorylated in nuclear extract, immobilized on Ni^{2+}-agarose and after removal of the extract aliquots were dephosphorylated by PP1 from rabbit skeletal muscle. This affinity matrix was then used to determine binding of bacterially expressed GST-SF2/ASF. As shown in Figure 4C, the dephosphorylated tra2-beta1 protein exhibited a higher affinity toward SF2/ASF. This reflects the *in vivo* situation where tra2-beta1 wild-type binds to SF2/ASF and tra2-beta1 whereas the tra2-beta1-RATA mutant shows no interaction. We did not observe residual PP1 binding prior to loading SF2/ASF to the tra2-beta1 affinity matrix, indicating that the effect is phosphorylation-mediated and does not reflect a tethering activity of PP1 (Fig. 4C). Furthermore, we did not observe binding of GST to tra2-beta1 bound to the matrix under any experimental conditions (Supplementary Material, Fig. S2B). These data indicate that the dephosphorylation of tra2-beta1 by PP1 promotes the multimerization between tra2-beta1 and its interacting proteins.

PP1 regulates the usage of alternative exons

Tra2-beta1 regulates alternative exons by binding to a characteristic, degenerate, but purine-rich sequence that often acts as an exonic enhancer (9,10) and we next asked whether PP1 could regulate such exons. Experimentally, it was shown that in a concentration-dependent manner tra2-beta1 promotes inclusion of its own exon 2, tau exon 10 and SMN2 exon 7 (10). Since the molecular interactions of tra2-beta1 were influenced by PP1-mediated dephosphorylation, we tested these exons for their dependency on PP1 activity. We employed established minigene systems where each alternative exon is flanked by its constitutive exons in a reporter gene construct. This reporter construct is cotransfected with expression vectors for *trans*-acting factors and their influence on alternative splicing is determined by RT–PCR (54). NIPP1 (nuclear inhibitor of protein phosphatase-1) is a specific inhibitor of PP1 (55). We therefore cotransfected reporter-minigenes containing tra2-beta1-dependent alternative exons together with either PP1cgamma or NIPP1 expression clones into HEK293 cells, which increased or decreased cellular PP1 activity (55). We determined the influence of PP1 activity on alternative splicing by RT–PCR (54). As shown in Figure 4D–F, an increase in PP1 expression promoted the exclusion of tra2-beta1-dependent exons. In contrast, the inhibition of nuclear PP1 by the expression of NIPP1 promoted tra2-beta1-dependent exon inclusion. The effect on exon usage was proportional to the increase in the level of PP1cgamma and NIPP1 protein that were detected by western blot from the transfected cells (Fig. 4G). To further rule out non-specific effects, we decreased the concentration of PP1 by performing RNA interference. We reduced the amount of the three endogenous PP1 isoforms, PP1alpha, beta and gamma, by co-transfecting three pairs of siRNAs with the reporter minigenes. As shown in Figure 5A–C, decreasing the PP1 concentration with siRNA had an effect similar to blocking PP1 activity with NIPP1, whereas a control siRNA had no influence on splice site selection. Again, the effect on splice site selection was proportional to the decrease of PP1 (Fig. 5D). The effect of PP1 reduction by siRNA is less pronounced than reducing PP1 activity by NIPP1 overexpression (Fig. 4D–G), which most likely reflects that all three PP1 isoforms have to be silenced simultaneously in the transfection experiments.

The effect of PP1 activity on SMN2 exon 7 usage (Figs 4F and 5C) is of medical importance, since promoting exon 7 usage would be beneficial for children with SMA (38). We therefore concentrated on this exon, and investigated whether the effect of PP1cgamma is dependent on its catalytic activity or is due to sequestration of tra2-beta1 protein by forming a splicing-inactive PP1 : tra2-beta1 complex. We compared the action of PP1 with its binding mutant PP1-F257A, which is mutated in the hydrophobic channel that mediates the binding to RVXF-motifs and with PP1-H125A that is catalytically inactive (47). In contrast to the wild-type form, the F257A-binding mutant and the catalytically inactive mutant H125A had no effect, demonstrating that binding and subsequent dephosphorylation is necessary for the effect of PP1 on splice site selection (Fig. 5E). Finally, we compared the influence of tra2-beta1 and tra2-beta1-RATA on exon 7 inclusion. Whereas tra2-beta1 increases exon 7 inclusion in a concentration-dependent manner, comparable amounts of the RATA mutant protein lead to exon skipping (Fig. 5F), most likely because tra2-beta1-RATA substitutes at higher concentration endogenous tra2-beta1 on SMN2. Since tra2-beta1-RATA does not bind to other SR-proteins (Fig. 4A–C), the recognition of exon 7 is abolished. This demonstrates that the exact control of tra2-beta1 dephosphorylation by PP1 is necessary for proper action of tra2-beta1.

Several splicing factors bind to PP1 via a phylogenetically conserved RVXF motif located on the beta-4 sheet of the RRM

Next, we determined whether blocking PP1 activity has an effect on splice site selection of endogenous genes. We constructed an oligonucleotide array that contained all known alternative splice variants from splicing factors, as well as

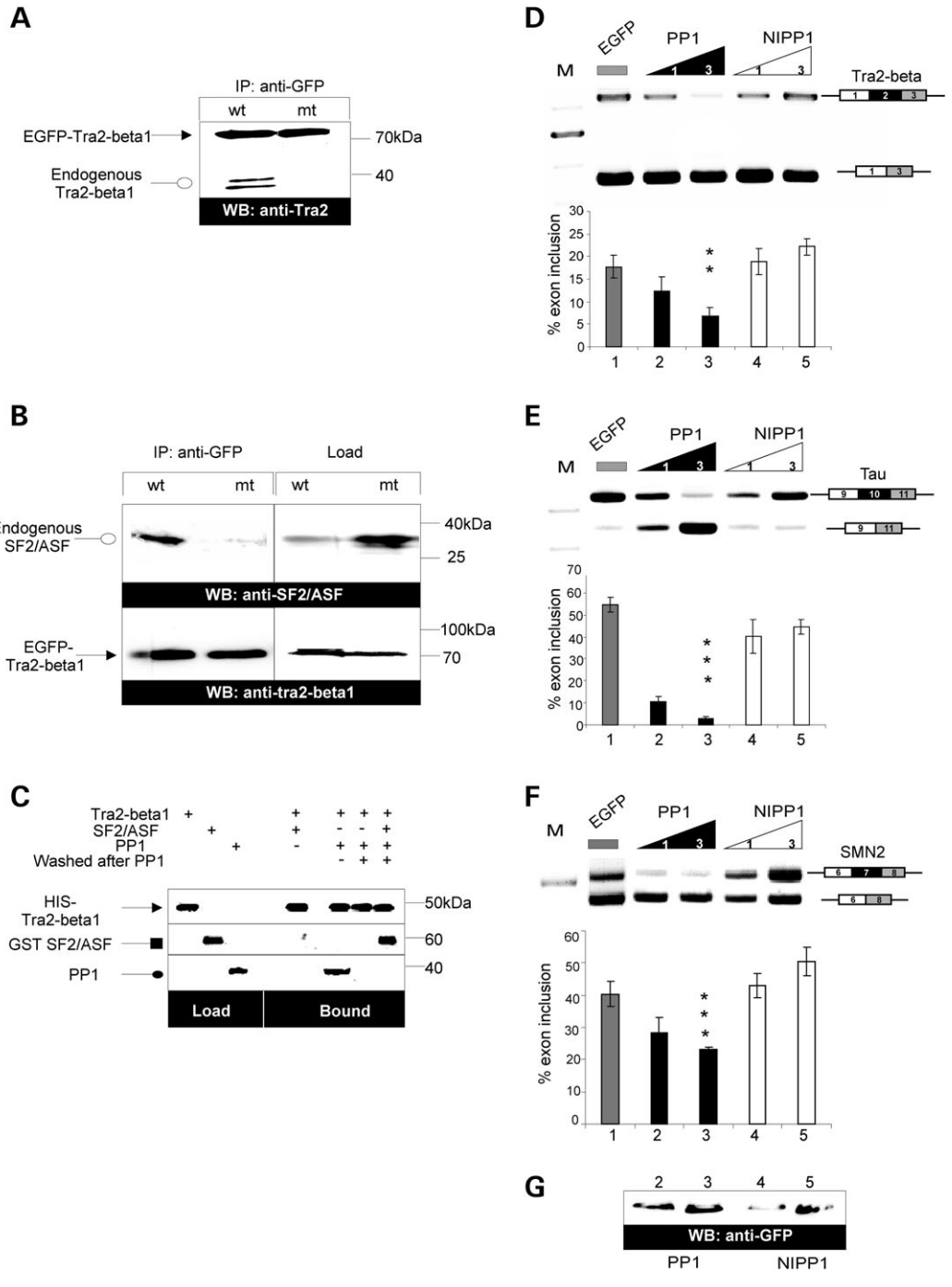

Figure 4. PP1-dependent phosphorylation controls protein interactions of tra2-beta1 and alternative splice site selection – (**A**) PP1-dependent homomultimerization of tra2-beta1: EGFP-tagged wild-type and EGFP-tra2-beta1-RATA was expressed in HEK293 cells. Protein complexes were recovered by immunoprecipitation with anti-GFP antisera. Endogenous tra2-beta1 binding to these proteins was detected with a pan-tra2-beta1 antiserum (7). Round arrow: endogenous tra2-beta1, pointed arrow: EGFP-tagged tra2-beta1. Tra2-beta1 migrates as two bands that are differently phosphorylated (19). (**B**) PP1-dependant heteromultimerization of tra2-beta1: EGFP-tagged wild-type and EGFP-tra2-beta1-RATA containing protein complexes were isolated as in (A). Top row: endogenous SF2/ASF was identified with anti-SF2/ASF; bottom row: reblot with anti-tra2-beta1. (**C**) Phosphorylation-dependent interaction between recombinant tra2-beta1 and SF2/ASF. His-tra2-beta1 was immobilized on Ni^{2+}-agarose and the binding of recombinant GST-SF2/ASF was determined without or after PP1 treatment, as indicated on top. 'Washed after PP1' indicates that prior to loading SF2/ASF, the tra2-beta1 affinity matrix was washed and no PP1 could be detected (load: SF2/ASF loaded on column). (**D**–**F**) An increasing amount of expression clones for PP1 and its nuclear inhibitor NIPP1 was cotransfected with the indicated reporter minigenes containing tra2-beta1-dependent exons. The alternative splicing of each reporter gene was determined by RT–PCR, as previously described (10,38,83). A representative ethidium-bromide stained gel of each experiment is shown. Under each experiment, the statistical evaluation of at least four independent experiments is shown. The numbers in the triangle represent μg of expression construct transfected into 3×10^5 cells. (D) Tra2-beta, exon 2; (E) tau, exon 10; (F) SMN2, exon 7. Stars indicate *P*-values from student's test, when mock-transfected (lane 1) and PP1 transfected cells (lane 2) were compared (tra2-beta: $P=0.004$; SMN: $P=0.001$; tau: $P=0.0005$). (**G**) Expression analysis after cotransfection. Representative western blots show the expression of the transfected EGFP-PP1cgamma and EGFP-NIPP1. The numbers on top correspond to the lanes in the experiments D–F.

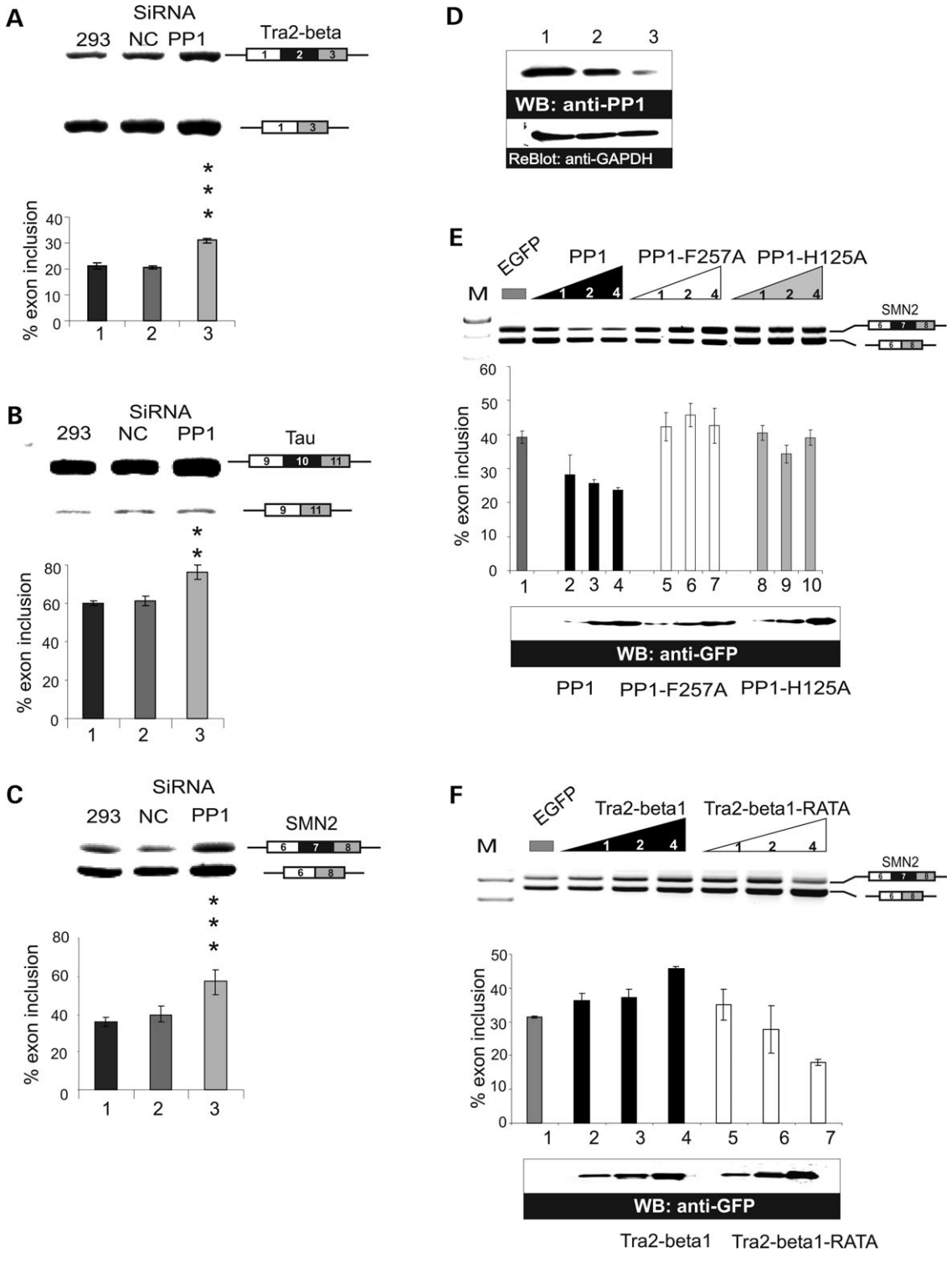

Figure 5. PP1 regulation of alternative exon usage – (**A**–**C**) The expression of PP1 was reduced by cotransfecting siRNA against all PP1 isoforms with the reporter minigenes. 293: cells were treated only with the transfection reagent; NC: non-specific (pBluescript) siRNA; PP1: siRNA against all three PP1 isoforms. (A) Tra2-beta, exon 2; (B) tau, exon 10; (C) SMN2, exon 7. Stars indicate *P*-values from student's test, when mock-transfected (lane 2) and PP1-transfected cells (lane 3) were compared (tra2-beta: $P=0.00015$; SMN: $P=0.002$; tau: $P=0.0006$). (**D**) Representative western blot detecting the expression of endogenous PP1 and its reduction by siRNA. The numbers on top correspond to the lanes in the experiments A–C. (**E**) The SMN2 reporter minigene was cotransfected with an increasing amount of PP1cgamma expression constructs, an expression construct encoding the binding mutant F257A, or the catalytically dead H125A mutant. The western blot below the statistical evaluation shows the accumulation of transfected PP1cgamma and PP1-F257A, and PP1-H125A in the HEK293 cells. The lanes of the western blot correspond to the lanes in the statistical evaluation. (**F**) The SMN2 reporter minigene was cotransfected with an increasing amount of tra2-beta1 expression constructs or an expression construct encoding the tra2-beta1-RATA mutant. The western blot shows the accumulation of transfected tra2-beta1 and tra2-beta1-RATA. The lanes of the western blot correspond to the lanes in the statistical evaluation.

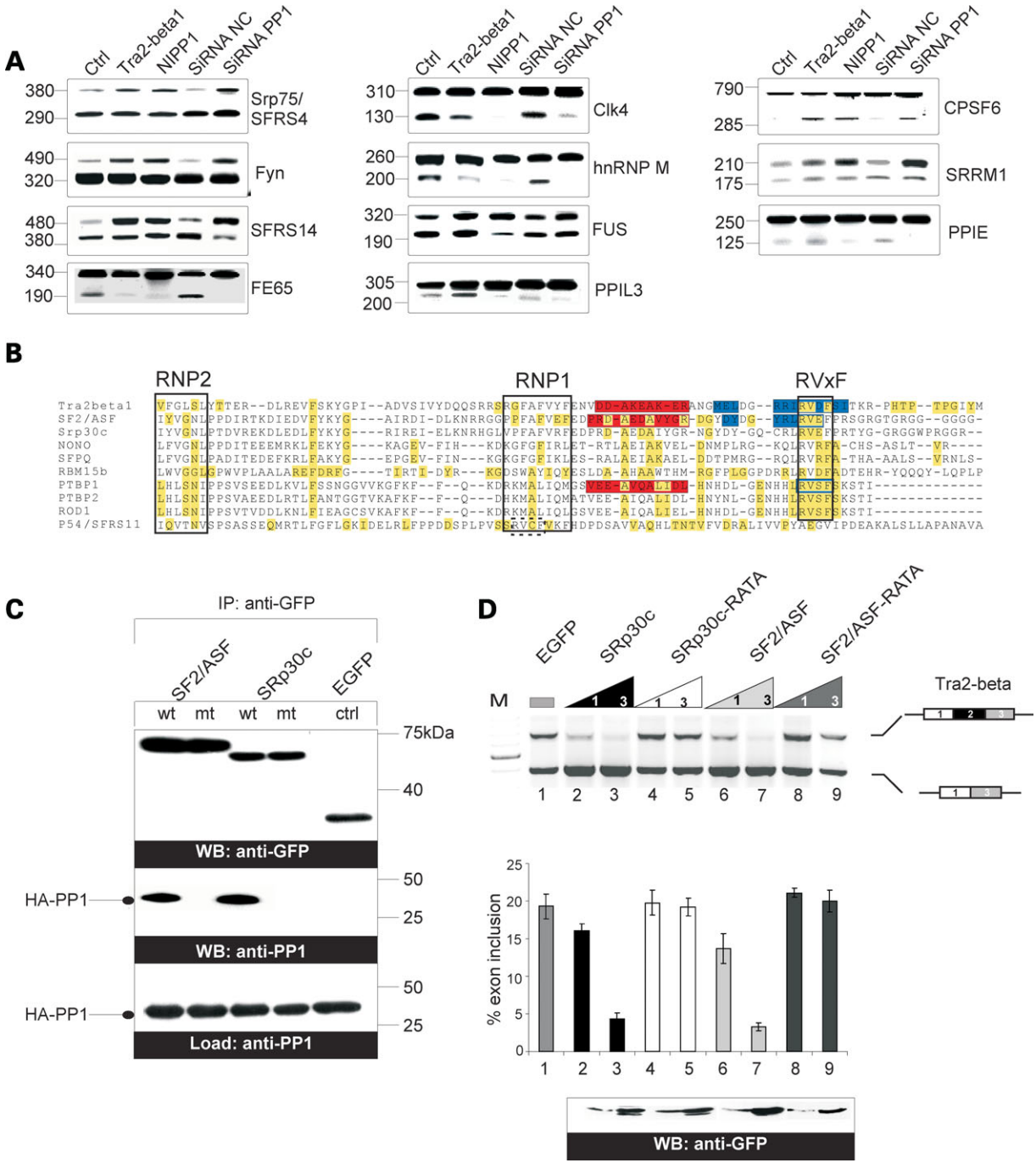

Figure 6. The PP1 docking motif is found in other RRMs – (**A**) Validation of array analysis by RT–PCR. EGFP-tra2-beta1 or EGFP-NIPP1 was transiently overexpressed in HEK293 cells, or cells were treated with mock siRNA (siRNA NC), or a mixture of siRNAs against all PP1c isoforms (siRNA PP1). Splicing events identified by splicearray analysis (Supplementary Material, Fig. S3) were amplified by RT–PCR using primers in the flanking constitutive exons. (**B**) The alignment shows the RRMs of the human proteins indicated. RNP2, RNP1 and the RVXF PP1-binding motif are boxed. The proteins are SFRS10 (tra2-beta1), SF2/ASF, SRp30c, SRp54/SFRS11, p54nrb (NONO) (84,85), SFPQ (86), RBM15 (87,88), PTB (89), nPTB (90) and ROD1 (91). Amino acids that are fully evolutionary conserved in each protein are marked in yellow. The known structural elements of tra2-beta1, SF2/ASF and PTB are indicated (red: alpha helix, blue: beta strand, conserved amino acids in these structures are marked in yellow and underlined). The RVEF motif in SF2/ASF is located in the beta-4 sheet, which is preceded by two small beta strands in RRM loop 5. The RVCF motif in p54/SFRS11 is located in the RNP1 and is indicated by a dotted box. (**C**) PP1 binding depends on the RVEF motif present in SF2/ASF and SRp30c. EGFP-tagged SF2/ASF and SRp30c was expressed in HEK293 cells together with HA-PP1 and immunoprecipitated with anti GFP antibodies. Wt: RVEF, mt: RVEF changed to RATA. The presence of HA-PP1 in the immunoprecipitates was determined by western blot. Load: western blot using material from the cellular lysates. (**D**) The ability of SF2/ASF and SRp30c to influence tra2-beta1 exon 2 inclusion depends on the RVEF motif. The gel shows the RT–PCR analysis of a transfection assays using a tra2-beta reporter gene and expression constructs of the EGFP-tagged proteins indicated. The western blot detects expression of the transfected proteins.

some well-studied model systems. The alternative splicing events were detected by a combination of exon-junction and exon body probes, as previously described (56). First, we compared the mRNA isolated from untreated HEK293 cells with cells where tra2-beta1 was overexpressed. Dye-swap experiments showed strong probe variation (correlation coefficient = 0.75 and 0.56, Supplementary Material, Fig. S6). We therefore used the array as an exploration tool and verified findings by RT–PCR. The fold-changes in the array analysis indicated that 65 out of a total of 942 alternative splicing events were strongly influenced by tra2-beta1 concentration (Supplementary Material, Fig. S3). We tested 18 of these events and confirmed for 11 alternative exons their dependency on tra2-beta1 by RT–PCR, using primers in the flanking constitutive exons (Fig. 6A). With the exception of alternative exons in CPSF6, PPIL3 and PPIE, tra2-beta1 overexpression promotes exon inclusion, supporting earlier findings that the protein acts as a general activator of exons (9,10). We then compared overexpression of tra2-beta1 with inhibition of PP1 by NIPP1 in HEK293 cells. In most cases where we could confirm the array data by RT–PCR, we found that blocking PP1 activity has a similar effect on alternative splice site selection as increasing the tra2-beta1 concentration (Fig. 6A). To further rule out effects from overexpression, we removed all three PP1 isoforms by siRNA. As shown in Figure 6A (right panels), siRNA treatment had an effect similar to NIPP1 overexpression, demonstrating that the effect on splice site selection is mediated by PP1. These data show that PP1 activity, specifically regulated by NIPP1, can influence alternative splice site selection.

When compared to tra2-beta1, NIPP1 expression had in some cases (Clk4, FUS) a stronger effect on exon inclusion than tra2-beta1 overexpression and in two cases it had an opposite effect (PPIL3, PPIE) (Fig. 6A). Therefore, we investigated whether PP1 could also influence other splicing factors. Since the PP1-binding site of tra2-beta1 is located within the beta-4 strand of the RRM, we investigated whether other RRMs could function in PP1 binding. We examined all known proteins containing an RRM for the presence of the RVXF-binding consensus sequence. From 497 proteins analyzed, 12 contain the RVXF-binding motif. In two proteins, PABPC3 and RBM6, the RVXF motif is located outside of the RRM. In the remaining cases, the motif is located in RRM (Fig. 6B). In eight of the nine cases, the PP1-binding motif is within the beta-4 sheet and for p54/SFRS11, it is in RNP1. Proteins with a putative PP1-binding site in the RRM can be subdivided into SR-proteins and hnRNPs. In addition to tra2-beta1, the group of SR-proteins contains SF2/ASF, SRp30c and the related SRp54. The remaining hnRNPs p54nrb (NONO), PSF (SFPQ), nPTB and ROD1 are all structurally related to the PTB, hnRNP I. A further phylogenic analysis demonstrates that the motif is conserved throughout evolution in each protein (Supplementary Material, Fig. S4). The presence of a PP1-binding motif explains earlier findings that PSF binds to PP1 in yeast assays (57). Since an interaction between SR-proteins and PP1 has not been reported so far, we tested binding of PP1 to SF2/ASF and SRp30c by coimmunoprecipitation. As shown in Figure 6C, PP1 coimmunoprecipitates with SF2/ASF and SRp30c. However, when the PP1-binding motif RVEF present in both proteins is mutated to RATA, the coimmunoprecipitation is completely abolished. These data strongly suggest that PP1 binds to the beta-4 sheet of the RRM of SF2/ASF and SRp30c. We did not detect binding of PP1 to RATA mutants in the absence of benzonase which allows nucleic-acid : protein complexes to stay intact. This shows that the interaction between PP1 and SR-proteins depends only on protein : protein binding (Supplementary Material, Fig. S1C and D). Finally, we used the alternative spliced exon 2 of the tra2-beta pre-mRNA to test whether the interaction with PP1 is functional important for SF2/ASF and SRp30c. We showed previously that SRp30c and SF2/ASF abolish exon 2 inclusion by sequestering tra2-beta1 (10). As shown in Figure 6D, SRp30c-RATA and SF2/ASF-RATA have no effect on exon 2 inclusion in transfection assays, whereas the wild-type sequences promote exon 2 skipping, demonstrating that binding of PP1 is important for the function of these splicing factors. These data show that PP1 regulates the activity of several splicing factors after binding to a phylogenetic conserved motif located on their RRM.

PP1 inhibitors promote the formation of exon 7 containing SMN mRNA, SMN protein and gems *in vivo*

A number of cell permeable protein phosphatase inhibitors including tautomycin, microcystin, calyculin A and cantharidin can be used to study the role of protein phosphatases 1 and 2 in intact cells and we investigated whether these compounds would interfere with splice site selection. We tested these inhibitors in HEK293 cells that were transfected with the SMN2 reporter minigene. We observed a significant inclusion of exon 7 with all these inhibitors, but the effect was most pronounced with tautomycin, which inhibits PP1 more potently than PP2A and other phosphatases. In contrast, we did not see SMN2 exon 7 inclusion with the protein tyrosine phosphatase inhibitor dephostatin, or the PP2A inhibitors fostriecin or nodularin (58). This indicates that blocking endogenous PP1 activity by chemical agents can promote SMN2 exon 7 inclusion (Fig. 7A).

So far, we analyzed the effect of PP1 on splice site selection in systems using overexpression of proteins and reporter genes. To analyze the effect of PP1 in an endogenous system, we employed primary fibroblast cell lines from persons with SMA types I–III. In these cells, both alleles of the SMN1 gene are deleted, but the SMN2 gene is still present. These cells were treated with 10 nM of the PP1 inhibitor tautomycin. Subsequently, exon 7 containing SMN mRNA was amplified using primers in exons 6 and 8. GAPDH was coamplified in the same reaction and served as a loading control. As shown in Figure 7B, this treatment resulted in an increase in mRNA containing exon 7. Since the SMN1 gene is absent in these cells, this increase in exon 7 containing mRNA can be only explained by a change in processing of mRNA derived from the SMN2 gene. We then determined whether there was an effect on the SMN protein and detected the endogenous SMN protein by western blot analysis. In agreement with the change in alternative splicing, we observed an accumulation of SMN protein after tautomycin treatment (Fig. 7C).

Within the nucleus, SMN localizes to discrete granules known as gems. The number of nuclei with gems and the

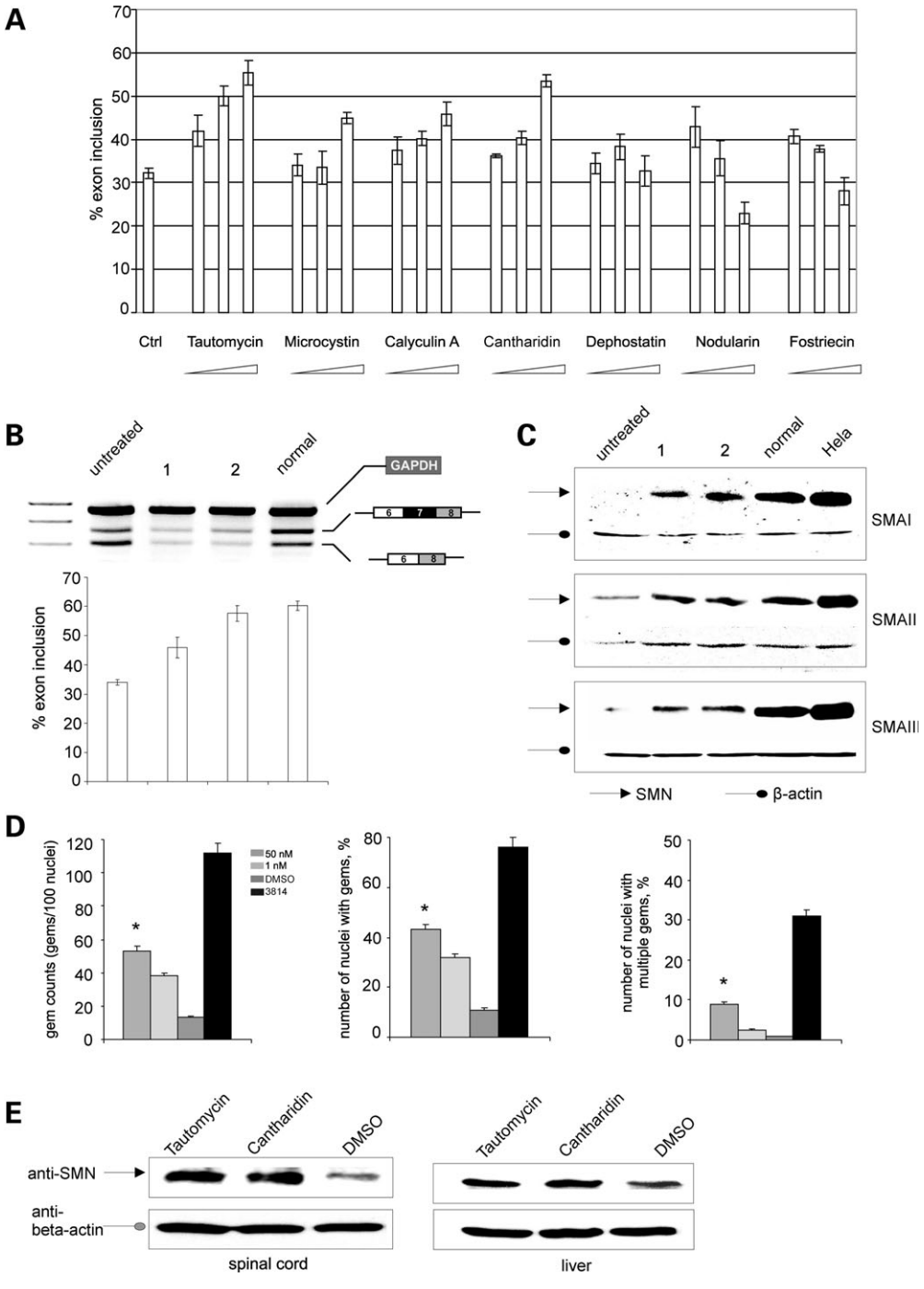

Figure 7. PP1 Inhibitors regulate endogenous SMN2 exon 7 – (**A**) Effect of different PP1 inhibitors on SMN exon 7 usage. HEK293 cells were transiently transfected with the SMN2 reporter minigene and treated with an increasing concentration of the protein phosphatase inhibitors. Phosphatase inhibitors are arranged according to their specificity for PP1. Tautomycin has the highest specificity to block PP1; dephostatin is a tyrosine phosphatase inhibitor with low affinity to PP1. (**B**) Tautomycin causes accumulation of SMN2 mRNA containing exon 7 in fibroblasts from children with type I SMA. Fibroblasts from a child with type I SMA that lack SMN1 were treated with tautomycin and the resulting RNA was analyzed by RT–PCR after 1 and 2 days. GAPDH was co-amplified in the same reaction as an internal loading control. The graph underneath the representative ethidium bromide stained gel shows the statistical evaluation of four independent experiments. (**C**) Tautomycin causes accumulation of SMN protein in SMA fibroblasts from type I–III patients. Cells were treated with 10 nM tautomycin from 1 to 2 days and cell lysates were analyzed using antisera against SMN, which detects the signal indicated by the pointed arrow. Round arrow: signal from beta-actin used as a loading control; normal arrow: lysates from non-transformed human control fibroblast; HeLa: lysates from HeLa cells. (**D**) PP1 inhibition causes gem formation. SMN1−/− patient fibroblasts were treated with tautomycin doses indicated. After 5 days gem formation was analyzed. Left: gem count (number of gems); middle: number of nuclei with gems; right: number of nuclei with multiple gems. SMN1−/− patient fibroblasts were compared with an SMN carrier cell line (3814, SMN1+/−). (**E**) Tautomycin and cantharidin cause accumulation of SMN protein in $Smn2^{+/+}$;$mSmn^{+/+}$ mice. Mice were treated with intraperitoneal injections of cantharidin or tautomycin. Spinal cord and liver tissue were analyzed 6 h later using antisera that detects only the human SMN protein. We and others have previously observed an SMN doublet when tissue samples are homogenized in SDS buffer and then frozen and thawed as opposed to being applied directly to the SDS gels. Actin was used to demonstrate equal loading.

number of gems per cell is reduced in SMA cells (59). SMA patient fibroblasts were treated with increasing doses of tautomycin (1–50 nM) for 5 days after which the number of nuclei with gems as well as the number of gems were counted. As a comparison, the number of nuclei with gems and the number of gems per 100 nuclei were also measured in fibroblasts derived from an SMA carrier (line 3814). Tautomycin-treatment increased both the number of gems (Fig. 7D, left) and the number of cells with gems (Fig. 7D, middle) in a dose-dependent manner. The number of nuclei with more than one gem also significantly increased in a dose-dependent manner after tautomycin treatment (Fig. 7D, right). As an example, 50 nM tautomycin elevates the number of gems by ~4.2-fold (53.0 ± 2.1; $n = 3$; $P < 0.001$). The data show that PP1 inhibition results in the production of SMN protein, which accumulates in the correct cellular compartment.

To test the effect of PP1 inhibition on exon 7 usage in an intact organism, we tested PP1 inhibitors in transgenic mice harboring human SMN2 genomic DNA (60). These mice contain two copies of the human SMN2 and two copies of the mouse SMN gene ($SMN2^{+/+}$; $mSmn^{+/+}$). The mice were intraperitoneally (i.p) given tautomycin (0.5 mg/kg) or cantharidin (0.1 mg/kg). The doses administered were at least one order of magnitude lower than the EC50s for these compounds [5 mg/kg for tautomycin (61) and 1 mg/kg for cantharidin (62)] when administered i.p. Additionally, none of the mice tested experienced any overt signs of distress during this study. Six hours later, spinal cord and liver tissue was analyzed by western blot. We used an antibody specific for human SMN protein for detection. As shown in Figure 7E, inhibition of endogenous PP1 caused an accumulation of human SMN protein in both the liver and the spinal cord of treated mice, demonstrating that PP1 inhibition can change splice site selection in an organism. Together, these data show that reducing the activity of endogenous PP1 promotes inclusion of the endogenous SMN exon 7.

DISCUSSION

PP1 binds to the RNA recognition motif of several splicing factors

Previous work on SR-protein kinases has demonstrated the importance of SR-protein phosphorylation for alternative splice site selection (63–66). The phosphorylation influences the affinity between SR-proteins, which could regulate the formation of protein-complexes on the pre-mRNA that identify exons (24). Furthermore, it was shown that dephosphorylation of SF2/ASF and possibly other SR-proteins are necessary for the splicing reaction to occur after spliceosome assembly (29,31,67), showing that SR-protein function is regulated by interplay between kinases and phosphatases. However, the binding partners of the phosphatases in the spliceosome were unknown. Here we demonstrate that PP1 binds directly to the RRM of the splicing factor tra2-beta1. RRMs consist of about 90 amino acids arranged in a conserved structure containing four antiparallel beta strands connected by two alpha helices. The RRM functions mainly in binding single stranded RNA, but recently it was shown that it also acts as a protein : protein interaction domain (68). In almost all analyzed RRM : RNA structures, the RNA contacts directly only the central beta-1 and beta-3 sheets, while the external beta-4 and beta-2 sheets increase affinity and specificity by influencing the structure (68). Our database analyses showed that RRMs from at least 10 proteins contain the characteristic RVXF motif. Interestingly, the protein that is most closely related to tra2-beta1, tra2-alpha does not contain a predicted PP1-binding site. In eight of the nine RRM-containing proteins, the RVXF motif that docks to PP1 is in their predicted beta-4 sheets. This localization was also shown by the crystal structure of the RRM of PTB (69) and the NMR structures of SF2/ASF and tra2-beta1 (PDB: 1X4A, 2CQC). We showed that in addition to tra2-beta1, two other SR-proteins, SF2/ASF and SRp30c use it to bind to PP1. The crystal structure of PP1 with its regulatory G-subunit [G(M)] and computer simulation of PP1-binding partners indicated that most RVXF motifs interacting with the binding pocket of PP1 are in an extended beta sheet formation (40,42), suggesting that the structural arrangement of the RVXF docking motif in the beta-4 sheet of RRMs allows for binding to PP1.

These data show that binding to the catalytic subunit of protein phosphatase is an evolutionary conserved function of a subgroup of RRMs. The striking evolutionary conservation of the sequence and structure of the PP1 docking motif in splicing factors could further indicate a conserved interaction with the spliceosome. U2 and U5 snRNPs are regulated by PP1 action (33), but none of the particle components have known PP1-binding properties. It is possible that the PP1 activity acting on these snRNPs in the spliceosome is mediated by RNA-binding proteins with an RVXF-PP1 docking motif that binds to the pre-mRNA while being processed. Since the dephosphorylation of spliceosomal proteins is necessary for the spliceosomal cycle, this arrangement would allow the pre-mRNA that is processed to control the re-formation of the spliceosome. This model would explain our seemingly paradox observation that tra2-beta1-RATA protein which cannot bind to PP1 blocks exon 7 inclusion (Fig. 5F), whereas PP1 inhibition promotes SMN2 exon 7 inclusion (Fig. 4F). In the first case, PP1 cannot promote processing of exon 7, since the tra2-beta1-RATA mutant replaces tra2-beta1. In the second case, PP1 is present, but less active, which could promote alternative exon usage by regulating the processing rate. An influence of processing rate and splice site selection has been observed in the fibronectin system (70). Our array analysis indicated that most of the pre-mRNAs are not affected by the level of PP1 inhibition that we achieved in our experiments, suggesting that the response to PP1 is specific for pre-mRNAs and not a general decrease of spliceosomal activity. Inspection of the exons regulated by tra2-beta (Fig. 6A) shows that almost all of them contain a RAAG signature, which is characteristic for tra2-beta1 (10). One exception is PPIE, which contains no predicted tra2-beta1-binding site in the exon. However, the exon contains predicted binding sites for SF2/ASF and SC35, suggesting that tra2-beta1 acts on this exon indirectly by sequestering these proteins. The lack of direct tra2-beta1 binding could explain why this exon responds differently to tra2-beta1 and PP1.

PP1 regulates the function of tra2-beta1 by dephosphorylation

We showed that the direct result of PP1 binding to tra2-beta1 is a dephosphorylation of tra2-beta1. In agreement with earlier studies investigating hyperphosphorylation of SF2/ASF after kinase treatment, we found that the phosphorylation state of tra2-beta1 controls its binding to interacting proteins. Dephosphorylation of tra2-beta1 promotes its RS-domain-mediated homomultimerization and binding to SF2/ASF. When the RVDF docking motif is destroyed, these interactions are abolished, indicating that PP1 dephosphorylates sites in the RS-domains of tra2-beta1. We next tested whether PP1 activity can influence splice site selection, since the formation of transient protein complexes on exons is necessary for their proper recognition. PP1 activity was either increased by transfecting PP1c expression constructs or it was decreased by transfected NIPP1. NIPP1 is a nuclear protein that inhibits specifically PP1. In most cases analyzed, we found that a decrease of PP1 had a similar effect on alternative exon usage, as did the increase in the tra2-beta1 concentration. However, there are several cases of alternative exons that responded much stronger to NIPP than to tra2-beta1. This most likely indicates that other splicing factors that are dephosphorylated by PP1, such as SF2/ASF or SRp30c, are part of the protein complexes regulating these exons. We did not see an effect on splice site selection using PP1 mutants without phosphatase activity, showing that PP1 exerts its effect on splice site selection by dephosphorylation and not just by binding to an RRM.

The catalytic subunit of PP1 associates with numerous different proteins that can function as subcellular targeting proteins, substrate-specifiers or inhibitors. Cellular signal transduction pathways, for example cAMP-dependent activation of protein kinase A, regulate the binding of PP1 to these proteins. This explains why the subcellular localization of the regulatory subunits depends on the cell type and is highly dynamic in a given cell (71). The association of PP1 with regulatory proteins will affect its ability to dephosphorylate splicing factors with the PP1 docking motif. This could explain why alternative splice site usage in various cell types is often very different, although the concentration of regulatory factors is quite similar. Our data suggest that the phosphorylation state of splicing regulatory factors is as important as their relative concentration and that PP1 activity is a key component in this regulation.

PP1 inhibitors are potentially beneficial for treating diseases caused by pathophysiological splice site selection

A misregulation of alternative exons is observed in several diseases, among them Alzheimer's disease (72), breast cancer (13) and SMA (38). It would therefore be beneficial to develop therapeutic strategies that intervene with splice site selection. Since the cause of SMA is genetically clearly defined, we focussed on this disease. It was previously demonstrated that increasing the tra2-beta1 concentration or activity would cause inclusion of SMN exon 7 (38). We therefore tested the PP1 inhibitor tautomycin in patient cells and found that it promoted inclusion of exon 7 and caused the formation of SMN protein. Although the administration of PP1 inhibitors promoted exon 7 inclusion and SMN2 protein formation, we surprisingly saw a decrease in total SMN2 RNA relative to the internal GAPDH control (Fig. 7B). Since the RRM-containing proteins that bind to PP1 (Fig. 6B) regulate different aspects of pre-mRNA processing, it is likely that PP1 inhibition has additional effects, e.g. on RNA stability or RNA translation. SR-proteins have been shown to promote translation when bound to mRNAs (73,74) and we show that SF2/ASF activity is regulated by PP1 binding (Fig. 6C). It remains therefore to be determined whether PP1 acts on translation by regulating the phosphorylation state of SR-proteins attached to pre-mRNA. Administration of two PP1 inhibitors, tautomycin and cantharidin, to mice harboring the human SMN2 genomic transgene (60) resulted in an increase in SMN protein in spinal cord and liver, demonstrating that these compounds can alter exon usage after crossing the blood–brain barrier. This demonstrates that modulation of phosphatase activity can be used to alter alternative splice site selection *in vivo*. However, our array and RT–PCR analysis shows that PP1 inhibition causes a change in numerous exons. Tautomycin and cantharidin can be viewed as first generation, or proof of concept, drug candidates. We can use these compounds as chemical backbones to design more potent compounds with more desirable pharmacological properties, i.e. better oral bioavailability, lower toxicity, better blood–brain barrier penetration. Specificity for this new class of drugs could be achieved by combining PP1 inhibition with another therapeutic principle, e.g. with other drugs that affect exon 7 inclusion, such as valproic acid (75), by finding substances specific for the tra2-beta1 : PP1 complex, or by coupling PP1 inhibitors to nucleic acids binding to the desired target, similar to chimeras between RS-domains and antisense oligonucleotides (76).

MATERIALS AND METHODS

Immunoprecipitation and western blot

Immunoprecipitation and western blot were performed as described (77) using the anti-GFP (Roche) antibody. Western blot was performed with anti tra2 (pan tra2 beta) (10) 1 : 1000, anti PP1 (C-19) 1 : 200 (Santa-Cruz biotechnology), 7B10 anti-SMN 1 : 1000 (Santa-Cruz biotechnology), anti-GFP 1 : 5000 (Roche), and anti-beta-actin 1 : 1000, anti SF2/ASF 1 : 500 (Zymed Laboratories), Mouse anti-SMN mAb (4F11; 1 : 200) and a mouse anti-beta-actin mAb (clone AC40, Sigma-Aldrich; 1 : 15 000). The anti-SMN mAb reacts specifically with human SMN and was developed by Dr Christian Lorson (University of Missouri, Columbia, MO, USA). HRP-conjugated secondary antibodies were from either AP-Biotech Rockland Immunochemicals for Research or Santa Cruz Biotechnology and used in 1 : 10 000 dilution. In all experiments the protein in the 'load control' represents ~10% of the input protein for the immunoprecipitation.

Gel shift experiments

Gel shift experiments were performed as described (78). RNA was *in vitro* transcribed and 20 pmol of ^{32}P-labeled RNA were

incubated with protein for 15′ at 30°C. The mobility was tested in 6% native polyacrylamide gels. The transcribed RNA probe was GGCGACTGGGGGGTCAGGG.

Immunohistochemistry

Cos7 cells were grown on coverslips, transfected with pEGFP-tra2-beta1 and pECFP-PP1cgamma constructs overnight, washed in PBS at pH 7.4 and fixed in 4% para-formaldehyde for 20 min at 4°C. Fixed cells were washed three times in 1×PBS prior to mounting on microscope slides with Gel/Mount (Biomeda). The cells were examined by confocal laser scanning microscopy (Leica DMIRE2) using a HCX Plan Appochromat 100×1.4 CS oil immersion objective. For the simultaneous imaging of EGFP and ECFP fluorescence, both labels were exited with the 438 nm line of an argon laser and 488 nm line of a helium–neon laser, respectively. The emission from each flurochrome was detected using 465–514 nm (CFP) and 543–633 nm (GFP). We determined the mean distribution for each signal. Colocalization was defined when signals from both flurochromes were larger than the mean minus the standard deviation. The area of the cell was manually outlined and the degree of colocalization was determined using the Leica confocal software LCS v2.5/347.

Purification of tra2-beta1-His tag proteins

The tra-2beta1 pFastBac construct was generated by inserting tra2-beta1 cDNA into Hta (Invitrogen) vector. The purified plasmid DNA was transformed into DH10 Bac^{TM}, for transposition into the bacmid. SF9 cells were cultured at 28°C under serum-free conditions (TNM-FH medium, Becton-Dickenson). Cells were harvested at 48 h post-infection and expression of recombinant protein was analyzed by SDS-PAGE. The transfection into SF9 cells was performed in a 6-well format. At 48 h after infection, the SF9 cells were centrifuged at 500 *g* for 10 min and the pellet was resuspended in 1 ml of lysis buffer pH 7.8 (6 M Guanidine HCl, 20 mM Na_3PO_4 and 500 mM NaCl). The suspension was lysed with a 19 G hypodermic needle and centrifuged at 14 000 rpm in a 5417R (Eppendorf) for 25 min. The supernatant was then incubated for 1 h at 4°C with Ninitrilotriacetic acid (Ni-NTA) agarose beads (Qiagen) equilibrated with denaturing bind/wash buffer (8 M Urea, 20 mM $NaPO_4$, 500 mM NaCl, 0.1% Triton buffer pH 7.8). After incubation, the beads were loaded onto a column, washed with denaturing bind/wash buffer two times and native wash buffer (500 mM NaH_2PO_4, 300 mM NaCl, 20 mM Imidazol, 0.1% Triton pH 8.0) three times and eluted with native wash buffer containing 500 mM imidazole at 4°C.

Dephosphorylation assay of His-tra2-beta1 recombinant protein

The His-tra2-beta1 protein at concentrations of 1 mg/ml bound to a Ni-NTA resin was incubated in a typical reaction mixture of 60 μl containing HeLa nuclear extract, 0.3 μl, [gamma-^{32}P]ATP, (250 mCi/ml) (Hartmann Analytic), 25 mM $MgCl_2$, 3.3 mM Tris-acetate (pH 7.8), 6.6 mM potassium acetate, 1 mM magnesium acetate and 0.5 mM DTT for 30 min at 30°C. The samples were then washed in cold 1× PBS and 2× in native wash buffer containing 500 mM NaH_2PO_4, 300 mM NaCl, 30 mM Imidazol, 0.1% Triton pH 8.0. Half of the protein then was dephosphorylated with PP1, purified from rabbit skeletal muscle with a final concentration of 40 ng/μl in PP1 buffer (NEB). After collecting the resin by centrifugation, the supernatants were boiled in SDS sample buffer and subjected to electrophoresis in 12% polyacrylamide gels followed by Coomassie staining and western blotting.

In vivo splicing

Splicing assays and cotransfection were performed as described (54), employing the SMN2 minigene (38), containing the alternative exon 7 flanked by the constitutive exons 6 and 8 and the original introns, and SMN2 SE with exonic splicing enhancer mutated in the middle of exon 7 respectively (79). The MG Tra2 minigene is containing the alternative exon 2 flanked by the constitutive exons 1 and 3 (10) and the tau MG contains the alternative exon 10, flanked by exons 9 and 11 (27). Transfection of the minigenes was done in HEK293 cells. 1 μg of indicated minigenes were used together with increasing amounts of the indicated pEGFP-constructs and with the appropriate amount of empty pEGFP-C2 vector to ensure that equal amounts of DNA were transfected. The calcium phosphate method was used for transfection. RNA was isolated 16–18 h post-transfection by using the total RNA kit (Qiagen, Germany). Reverse transcription was performed in a total volume of 8.5 μl by using 2 μl RNA, 1 μl oligo (dT) (0.5 mg/ml), 1 μl first-strand buffer (Invitrogen, Germany), 10 mM DTT, 1 mM dNTP, five units SuperScript II RT (Invitrogen) at 42°C for 60 min. To ensure that only plasmid-derived minigene transcript was detected, subsequent amplification was performed with a vector-specific forward primer (pCI-forw: 5′-GGTGTCCACTCCCAGTTCAA) and the *SMN*-specific reverse primer SMNex8-rev (SMNex8-rev: 5′-GCCTCACCACCGTGCTGG) for SMN2 MG (79); with a vector specific primer pCR-RT-reverse (GCCCTCTAGACT CGAGCTCGA) and for the following PCR amplification primers, MGTra-F-Bam (GGGGATCCGACCGGCGCGTCG TGCGGGGCT) and MGTra-R-Xho (GGGCTCGAGTACCC GATTCCCAACATGACG) for Tra2-beta1 MG and with INS1 (cag cta cag tcg gaa acc atc agc aag cag) and antisense INS3 (cac ctc cag tgc caa ggt ctg aag gtc acc) for SV9/10L/11 Tau MG were used. PCR products resolved on ethidium bromide-stained agarose gels resulted in similar ratios. The ratio of exon inclusion to exon skipping was determined by using Image J program.

In vivo splicing assays with siRNAs

In vivo splicing assays with siRNAs were performed in a similar way. The siRNA knockdown of PP1 was done using HiPerfect Transfection Reagent (Qiagen, Hilden) using the reverse transfection procedure according to manufacturer's direction. siRNAs for PP1alpha, PP1beta and PP1gamma (Santa Cruz sc-36299, sc-36295, sc-36297) were used as a pan-siRNA mixture in 20 nM concentration. After 24 h 250 ng/well of the minigenes SMN2, tau and tra2-beta were

transfected as described earlier. After 40–42 h siRNA treatment (16–18 h after minigene transfection) RNA was isolated from 6×10^5 seeded cells. In parallel, cells were lysed in SDS-loading buffer for protein analysis (3×10^5 cells). One-tenth of the lysates was for western blot analysis using a mixture of antibodies against all PP1 isoforms. Analysis of minigenes was performed as described earlier.

Human cell lines and determination of gems

Cell lines derived from skin fibroblasts of a type I SMA patient (line 3813), a type II patient (2832), a type III patient (2873) and from a SMA carrier (line 3814) have been described previously (59) and were maintained in DMEM containing 10% (vol/vol) fetal bovine serum (Atlas), 2 mM glutamine (Invitrogen) and antibiotics (Invitrogen). For RT–PCR and immunoblot analyses, cells were plated into 12-well plates at a density of 4000 cells/cm^2. For immunofluorescence experiments, cells were seeded onto glass coverslips coated with 1% gelatin at a density of 4000 cells/cm^2. Drug compounds or DMSO were added to the medium at a 1 : 1000 dilution. Medium was changed daily and fresh compound was added. Immunostaining of fibroblast cells was accomplished as described previously (59) with modification. Briefly, cells grown on gelatinized coverslips were fixed with fixative buffer [2% para-formaldehyde, 400 μM $CaCl_2$, 50 mM sucrose in 100 mM sodium phosphate buffer, pH 7.4 (80)] for 30 min at room temperature, thoroughly rinsed with phosphate-buffered saline (PBS) and permeabilized with ice-cold acetone for 10 min. After drying for at least 30 min at room temperature, the cells were rehydrated with PBS for 10 min at room temperature and then blocked with 5 × BLOCK for 60 min at room temperature. The cells were incubated overnight with primary antibody solution (mouse anti-SMN mAb; MANSMA2 (8F7) (81) diluted 1 : 200 in 1 × BLOCK) at 4°C. The cells were then washed extensively (3 × 10 min) with PBS and incubated with secondary antibody solution (biotinylated goat anti-mouse IgG (Jackson ImmunoResearch) diluted 1 : 400 with 1 × BLOCK) for 60 min at room temperature. The cells were then washed with PBS (3 × 10 min) and then incubated with AlexaFluor 594-conjugated strepavidin (Invitrogen) diluted 1 : 200 with PBS for 60 min at room temperature. Cells were then counterstained with Hoechst 33342 (1 μg/ml) in PBS for 5 min. After thorough washing with PBS, coverslips were mounted onto glass slides with ImmuMount (Shandon Lipshaw) and stored at 4°C until analysis. For gem counting, immunolabeling was visualized using a Nikon fluorescent microscope and the number of gems in 100 randomly selected nuclei as well as the number of cells with gems were collected. Confocal images were obtained using a Zeiss 510 META Laser Scanning confocal microscope (Campus Microscopy and Imaging Facility, Ohio State University) as a series of optic sections (thickness of 500 nm/section) taken through the z-axis. These stacks of sections were then compressed using LSM 5 Image Browser (Carl Zeiss, Inc.). All parametric data were expressed as mean standard error. Comparisons made between parametric data were made using one-way ANOVA with a Bonferonni post hoc test. All statistical analyses were performed using SPSS v.15.

Array analysis

Five micro gram of total RNA were reverse transcribed in 30 μl with 200U Superscript II (Life Technologies), 4 μg random primers (Life Technologies) and final concentrations of dTTP and aa-dUTP of 250 μM, in 1 × first strand buffer (Life Technologies) at 42°C for 2 h. RNA strands were hydrolyzed with 10 μl NaOH (1 N) for 10 min at 65°C. The reaction mixtures were neutralized with 10 μl HCl (1 N). The resulting aa-cDNAs were next precipitated using 6 μl of NaAc, $3H_2O$ (3M) pH 5.2, 132 μl absolute ethanol, 0.5 μl glycogen and incubated over night at −20°C. aa-cDNA pellets were resuspended in 2.5 μl RNAse free water and labeled with 5 μl sodium bicarbonate (0.1 M) pH=9 and 2.5 μl Cyanine 3 or Cyanine 5 (Amersham Biosciences) in DMSO. Each sample was incubated in the dark for 1 h. The reactions were completed by adding 4.5 μl hydroxylamine (4 M) and incubated for 15 min. Labeled materials were purified using JetQuick PCR purification columns (GenoMed) as per manufacturer's instructions and eluted twice with 50 μl each of RNase free water preheated at 65°C. The cDNA yields and dye incorporation were quantified by spectrophotometry.

Hybridizations were performed using 2.5 μg of Cy3 and Cy5 labeled targets (for 11 K and 22 K slides respectively) along with 20 μg of herring sperm DNA (Invitrogen). The mixture was heated at 98°C for 3 min, and then brought to room temperature for 5 min in the presence of 25 μl of 10 × Control Targets from the *in situ* hybridization kit (Agilent Technologies). Following addition of the kit's 2 × hybridization buffer, the mixture was hybridized to the splicearrays at 65°C for 17 h.

The arrays were washed using Agilent's 60-mer Oligo Microarray Processing Protocol-SSPE Wash, with washes increased to 5 min each. All incubations were performed in an ozone-free atmosphere to prevent any degradation of signal. The arrays were scanned using Agilent's Microarray Scanner. The images were analyzed with Feature Extraction software, version 8.1 using all default settings.

The processed signals were imported into a Splicearray Analysis Tool (SAT), summarizing the probe data according to gene locus and splice event. The SAT tool also contains extensive annotations for each splice event that permits the sorting and filtering of the results by several parameters such as the type of splicing event, signal strength and fold-change between the two samples.

Administration of PP1 inhibitors to mice

Adult *Smn2*$^{+/+}$;*mSmn*$^{+/+}$ mice (82) on a FVB/N genetic background were used to determine the effect of PP1 inhibition on SMN2 expression *in vivo*. These mice were obtained from an internal breeding colony (at Ohio State University) but are commercially available from Jackson Laboratories (stock number 005024; *FVB.Cg-Tg(SMN2)89Ahmb Smn1*^{tm1Msd}). These mice were obtained from *Smn2*$^{+/+}$; *mSmn*$^{+/-}$ parents and were genotyped as described (82). Mice received either tautomycin (0.5 mg/kg), cantharidin (0.1 mg/kg), or an equivalent volume of vehicle (DMSO in all cases) i.p at a dose volume of 1 μl/g. The treated mice were euthanized 6 h after dosing and tissues were harvested

and rapidly frozen in N_2. Tissues were stored at −80°C until use. All experiments were conducted in accordance with the protocols described in the National Institutes of Health *Guide for the Care and Use of Animals* and were approved by the Ohio State University Institutional Laboratory Animal Care and Use Committee.

SUPPLEMENTARY MATERIAL

Supplementary Material is available at HMG Online.

ACKNOWLEDGEMENTS

GST-SF2/ASF was kindly supplied by Cyril Bourgeois. We would like to thank Dr Glenn E. Morris for generously providing the MANSMA2 (8F7) antibody and the Campus Microscopy and Imaging Facility (Ohio State University) for providing access to their confocal microscope.

Conflict of Interest statement. None declared.

FUNDING

This work was supported by the European Union, EURASNET (S.S., CBD), the German Research Council (S.S.), the BMBF (S.S.), the families of SMA (FSMA to S.S. and MERB), the German Cancer Aid (S.S.) and the National Institutes of Health (NIH grant 3860 to A.H.M.B.).

REFERENCES

1. Venter, J.C., Adams, M.D., Myers, E.W., Li, P.W., Mural, R.J., Sutton, G.G., Smith, H.O., Yandell, M., Evans, C.A., Holt, R.A. *et al.* (2001) The sequence of the human genome. *Science*, **291**, 1304–1351.
2. Lander, E.S., Linton, L.M., Birren, B., Nusbaum, C., Zody, M.C., Baldwin, J., Devon, K., Dewar, K., Doyle, M., FitzHugh, W. *et al.* (2001) Initial sequencing and analysis of the human genome. *Nature*, **409**, 860–921.
3. Stamm, S., Ben-Ari, S., Rafalska, I., Tang, Y., Zhang, Z., Toiber, D., Thanaraj, T.A. and Soreq, H. (2005) Function of alternative splicing. *Gene*, **344C**, 1–20.
4. Smith, C.W. and Valcarcel, J. (2000) Alternative pre-mRNA splicing: the logic of combinatorial control. *Trends Biochem. Sci.*, **25**, 381–388.
5. Maniatis, T. and Tasic, B. (2002) Alternative pre-mRNA splicing and proteome expansion in metazoans. *Nature*, **418**, 236–243.
6. Beil, B., Screaton, G. and Stamm, S. (1997) Molecular cloning of htra2-beta-1 and htra2-beta-2, two human homologs of tra-2 generated by alternative splicing. *DNA Cell Biol*, **16**, 679–690.
7. Nayler, O., Cap, C. and Stamm, S. (1998) Human transformer-2-beta gene (SFRS10): complete nucleotide sequence, chromosomal localization, and generation of a tissue-specific isoform. *Genomics*, **53**, 191–202.
8. Dauwalder, B., Amaya-Manzanares, F. and Mattox, W. (1996) A human homologue of teh Drosophila sex determination factor transformer-2 has conserved splicing regulatory functions. *Proc. Natl Acad. Sci. USA*, **93**, 9004–9009.
9. Tacke, R., Tohyama, M., Ogawa, S. and Manley, J.L. (1998) Human Tra2 proteins are sequence-specific activators of pre-mRNA splicing. *Cell*, **93**, 139–148.
10. Stoilov, P., Daoud, R., Nayler, O. and Stamm, S. (2004) Human tra2-beta1 autoregulates its protein concentration by influencing alternative splicing of its pre-mRNA. *Hum. Mol. Genet.*, **13**, 509–524.
11. Forch, P. and Valcarcel, J. (2003) Splicing regulation in Drosophila sex determination. *Prog. Mol. Subcell Biol.*, **31**, 127–151.
12. Marin, I. and Baker, B.S. (1998) The evolutionary dynamics of sex determination. *Science*, **281**, 1990–1994.
13. Watermann, D.O., Tang, Y., zur Hausen, A., Jäger, M., Zhang, Z., Stamm, S. and Stickeler, E. (2006) Splicing factor Tra2-{beta}1 is specifically induced in breast cancer and regulates alternative splicing of the CD44 gene. *Cancer Res.*, **66**, 4774–4780.
14. Fischer, D.C., Noack, K., Runnebaum, I.B., Watermann, D.O., Kieback, D.G., Stamm, S. and Stickeler, E. (2004) Expression of splicing factors in human ovarian cancer. *Oncol. Rep.*, **11**, 1085–1090.
15. Matsuo, N., Ogawa, S., Imai, Y., Takagi, T., Tohyama, M., Stern, D. and Wanaka, A. (1995) Cloning of a novel RNA binding polypeptide (RA301) induced by hypoxia/reoxygenation. *J. Biol. Chem.*, **270**, 28216–28222.
16. Daoud, R., Mies, G., Smialowska, A., Oláh, L., Hossmann, K. and Stamm, S. (2002) Ischemia induces a translocation of the splicing factor tra2-beta1 and changes alternative splicing patterns in the brain. *J. Neurosci.*, **22**, 5889–5899.
17. Segade, F., Claudio, E., Wrobel, K., Ramos, S. and Lazo, P.S. (1995) Isolation of nine gene sequences induced by silica in murine macrophages. *J. Immunol.*, **154**, 2384–2392.
18. Tsukamoto, Y., Matsuo, N., Ozawa, K., Hori, O., Higashi, T., Nishizaki, J., Tohnai, N., Nagata, I., Kawano, K., Yutani, C. *et al.* (2001) Expression of a novel RNA-splicing factor, RA301/Tra2beta, in vascular lesions and its role in smooth muscle cell proliferation. *Am. J. Pathol.*, **158**, 1685–1694.
19. Daoud, R., Da Penha Berzaghi, M., Siedler, F., Hubener, M. and Stamm, S. (1999) Activity-dependent regulation of alternative splicing patterns in the rat brain. *Eur. J. Neurosci.*, **11**, 788–802.
20. Stamm, S. (2002) Signals and their transduction pathways regulating alternative splicing: a new dimension of the human genome. *Hum. Mol. Genet.*, **11**, 2409–2416.
21. Shin, C. and Manley, J.L. (2004) Cell signalling and the control of pre-mRNA splicing. *Nat. Rev. Mol. Cell. Biol.*, **5**, 727–738.
22. Shin, C., Feng, Y. and Manley, J.L. (2004) Dephosphorylated SRp38 acts as a splicing repressor in response to heat shock. *Nature*, **427**, 553–558.
23. Hagiwara, M. (2005) Alternative splicing: a new drug target of the post-genome era. *Biochim. Biophys. Acta*, **1754**, 324–331.
24. Xiao, S.H. and Manley, J.L. (1997) Phosphorylation of the ASF/SF2 RS domain affects both protein–protein and protein–RNA interactions and is necessary for splicing. *Genes Dev.*, **11**, 334–344.
25. Xiao, S.-H. and Manley, J.L. (1998) Phosphorylation–dephosphorylation differentially afects activities of splicing factor ASF/SF2. *EMBO J.*, **17**, 6359–6367.
26. Prasad, J., Colwill, K., Pawson, T. and Manley, J. (1999) The protein kinase Clk/Sty directly modulates SR protein activity: both hyper- and hypophosphorylation inhibit splicing. *Mol. Cell. Biol.*, **19**, 6991–7000.
27. Hartmann, A.M., Rujescu, D., Giannakouros, T., Nikolakaki, E., Goedert, M., Mandelkow, E.M., Gao, Q.S., Andreadis, A. and Stamm, S. (2001) Regulation of alternative splicing of human tau exon 10 by phosphorylation of splicing factors. *Mol. Cell. Neurosci.*, **18**, 80–90.
28. Kanopka, A., Muhlemann, O., Petersen-Mahrt, S., Estmer, C., Ohrmalm, C. and Akusjarvi, G. (1998) Regulation of adenovirus alternative RNA splicing by dephosphorylation of SR proteins. *Nature*, **393**, 185–187.
29. Cao, W., Jamison, S.F. and Garcia-Blanco, M.A. (1997) Both phosphorylation and dephosphorylation of ASF/SF2 are required for pre-mRNA splicing in vitro. *Rna*, **3**, 1456–1467.
30. Mermoud, J.E., Cohen, P. and Lamond, A.I. (1992) Ser/Thr-specific protein phosphatases are required for both catalytic steps of pre-mRNA splicing. *Nucleic Acids Res.*, **20**, 5263–5269.
31. Murray, M.V., Kobayashi, R. and Krainer, A.R. (1999) The type 2C ser/thr phosphatase PP2Cgamma is a pre-mRNA splicing factor. *Genes Dev.*, **13**, 87–97.
32. Deckert, J., Hartmuth, K., Boehringer, D., Behzadnia, N., Will, C.L., Kastner, B., Stark, H., Urlaub, H. and Luhrmann, R. (2006) Protein composition and electron microscopy structure of affinity-purified human spliceosomal B complexes isolated under physiological conditions. *Mol. Cell. Biol.*, **26**, 5528–5543.
33. Shi, Y., Reddy, B. and Manley, J.L. (2006) PP1/PP2A phosphatases are required for the second step of pre-mRNA splicing and target specific snRNP proteins. *Mol. Cell.*, **23**, 819–829.
34. Krawczak, M., Reiss, J. and Cooper, D.N. (1992) The mutational spectrum of single base-pair substitutions in mRNA splice junctions of human genes: causes and consequences. *Hum. Genet.*, **90**, 41–54.
35. Faustino, N.A. and Cooper, T.A. (2003) Pre-mRNA splicing and human disease. *Genes Dev.*, **17**, 419–437.

36. Stoilov, P., Meshorer, E., Gencheva, M., Glick, D., Soreq, H. and Stamm, S. (2002) Defects in pre-mRNA processing as causes of and predisposition to diseases. *DNA Cell Biol.*, **21**, 803–818.
37. Singh, N.N., Androphy, E.J. and Singh, R.N. (2004) The regulation and regulatory activities of alternative splicing of the SMN gene. *Crit. Rev. Eukaryot. Gene Expr.*, **14**, 271–285.
38. Hofmann, Y., Lorson, C.L., Stamm, S., Androphy, E.J. and Wirth, B. (2000) Htra2-beta 1 stimulates an exonic splicing enhancer and can restore full-length SMN expression to survival motor neuron 2 (SMN2). *Proc. Natl Acad. Sci. USA*, **97**, 9618–9623.
39. Cartegni, L., Hastings, M.L., Calarco, J.A., de Stanchina, E. and Krainer, A.R. (2006) Determinants of exon 7 splicing in the spinal muscular atrophy genes, SMN1 and SMN2. *Am. J. Hum. Genet.*, **78**, 63–77.
40. Egloff, M.P., Johnson, D.F., Moorhead, G., Cohen, P.T., Cohen, P. and Barford, D. (1997) Structural basis for the recognition of regulatory subunits by the catalytic subunit of protein phosphatase 1. *EMBO J.*, **16**, 1876–1887.
41. Bollen, M. (2001) Combinatorial control of protein phosphatase-1. *Trends Biochem. Sci.*, **26**, 426–431.
42. Meiselbach, H., Sticht, H. and Enz, R. (2006) Structural analysis of the protein phosphatase 1 docking motif: molecular description of binding specificities identifies interacting proteins. *Chem. Biol.*, **13**, 49–59.
43. Yang, J., Hurley, T.D. and DePaoli-Roach, A.A. (2000) Interaction of inhibitor-2 with the catalytic subunit of type 1 protein phosphatase. Identification of a sequence analogous to the consensus type 1 protein phosphatase-binding motif. *J. Biol. Chem.*, **275**, 22635–22644.
44. Wakula, P., Beullens, M., Ceulemans, H., Stalmans, W. and Bollen, M. (2003) Degeneracy and function of the ubiquitous RVXF motif that mediates binding to protein phosphatase-1. *J. Biol. Chem.*, **278**, 18817–18823.
45. Rafalska, I., Zhang, Z., Benderska, N., Wolff, H., Hartmann, A.M., Brack-Werner, R. and Stamm, S. (2004) The intranuclear localization and function of YT521-B is regulated by tyrosine phosphorylation. *Hum. Mol. Genet.*, **13**, 1535–1549.
46. Trinkle-Mulcahy, L., Sleeman, J.E. and Lamond, A.I. (2001) Dynamic targeting of protein phosphatase 1 within the nuclei of living mammalian cells. *J. Cell Sci.*, **114**, 4219–4228.
47. Lesage, B., Beullens, M., Nuytten, M., Van Eynde, A., Keppens, S., Himpens, B. and Bollen, M. (2004) Interactor-mediated nuclear translocation and retention of protein phosphatase-1. *J. Biol. Chem.*, **279**, 55978–55984.
48. Trinkle-Mulcahy, L., Andrews, P.D., Wickramasinghe, S., Sleeman, J., Prescott, A., Lam, Y.W., Lyon, C., Swedlow, J.R. and Lamond, A.I. (2003) Time-lapse imaging reveals dynamic relocalization of PP1gamma throughout the mammalian cell cycle. *Mol. Biol. Cell*, **14**, 107–117.
49. Winder, D.G. and Sweatt, J.D. (2001) Roles of serine/threonine phosphatases in hippocampal synaptic plasticity. *Nat. Rev. Neurosci.*, **2**, 461–474.
50. Bordelon, J.R., Smith, Y., Nairn, A.C., Colbran, R.J., Greengard, P. and Muly, E.C. (2005) Differential localization of protein phosphatase-1alpha, beta and gamma1 isoforms in primate prefrontal cortex. *Cereb. Cortex*, **15**, 1928–1937.
51. Nayler, O., Stamm, S. and Ullrich, A. (1997) Characterisation and comparison of four SR protein kinases. *Biochem. J.*, **326**, 693–700.
52. Leytus, S.P., Melhado, L.L. and Mangel, W.F. (1983) Rhodamine-based compounds as fluorogenic substrates for serine proteinases. *Biochem. J.*, **209**, 299–307.
53. MacKintosh, C. and Klumpp, S. (1990) Tautomycin from the bacterium Streptomyces verticillatus. Another potent and specific inhibitor of protein phosphatases 1 and 2A. *FEBS Lett.*, **277**, 137–140.
54. Stoss, O., Stoilov, P., Hartmann, A.M., Nayler, O. and Stamm, S. (1999) The in vivo minigene approach to analyze tissue-specific splicing. *Brain Res. Protoc.*, **4**, 383–394.
55. Beullens, M. and Bollen, M. (2002) The protein phosphatase-1 regulator NIPP1 is also a splicing factor involved in a late step of spliceosome assembly. *J. Biol. Chem.*, **277**, 19855–19860.
56. Fehlbaum, P., Guihal, C., Bracco, L. and Cochet, O. (2005) A microarray configuration to quantify expression levels and relative abundance of splice variants. *Nucleic Acids Res.*, **33**, e47.
57. Hirano, K., Erdodi, F., Patton, J.G. and Hartshorne, D.J. (1996) Interaction of protein phosphatase type 1 with a splicing factor. *FEBS Lett.*, **389**, 191–194.
58. Honkanen, R.E. and Golden, T. (2002) Regulators of serine/threonine protein phosphatases at the dawn of a clinical era? *Curr. Med. Chem.*, **9**, 2055–2075.
59. Coovert, D.D., Le, T.T., McAndrew, P.E., Strasswimmer, J., Crawford, T.O., Mendell, J.R., Coulson, S.E., Androphy, E.J., Prior, T.W. and Burghes, A.H. (1997) The survival motor neuron protein in spinal muscular atrophy. *Hum. Mol. Genet.*, **6**, 1205–1214.
60. Monani, U.R., Sendtner, M., Coovert, D.D., Parsons, D.W., Andreassi, C., Le, T.T., Jablonka, S., Schrank, B., Rossol, W., Prior, T.W. *et al.* (2000) The human centromeric survival motor neuron gene (SMN2) rescues embryonic lethality in Smn(−/−) mice and results in a mouse with spinal muscular atrophy. *Hum. Mol. Genet.*, **9**, 333–339.
61. Cheng, X.C., Kihara, T., Kusakabe, H., Magae, J., Kobayashi, Y., Fang, R.P., Ni, Z.F., Shen, Y.C., Ko, K., Yamaguchi, I. *et al.* (1987) A new antibiotic, tautomycin. *J. Antibiot. (Tokyo)*, **40**, 907–909.
62. Matsuzawa, M., Graziano, M.J. and Casida, J.E. (1987) Endothal and cantharidin analogues: relation of structure to herbicidal activity and mammalian toxicity. *J. Agric. Food Chem.*, **35**, 823–829.
63. Muraki, M., Ohkawara, B., Hosoya, T., Onogi, H., Koizumi, J., Koizumi, T., Sumi, K., Yomoda, J.I., Murray, M.V., Kimura, H. *et al.* (2004) Manipulation of alternative splicing by a newly developed inhibitor of Clks. *J. Biol. Chem*, **279**, 24246–24254.
64. Du, C., McGuffin, E., Dauwalder, B., Rabinow, L. and Mattox, W. (1998) Protein phosphorylation plays an essential role in the regulation of alternative splicing and sex determination in drosophila. *Mol. Cell*, **2**, 741–750.
65. Chalfant, C.E., Mischak, H., Watson, J.E., Winkler, B.C., Goodnight, J., Farese, R.V. and Cooper, D.R. (1995) Regulation of alternative splicing of protein kinase C beta by insulin. *J. Biol. Chem.*, **270**, 13326–13332.
66. Duncan, P.I., Stojkl, D.F., Marius, R.M. and Bell, J.C. (1997) In vivo regulation of alternative pre-mRNA splicing by the Clk1 protein kinase. *Mol. Cell. Biol.*, **17**, 5996–6001.
67. Mermoud, J.E., Cohen, P. and Lamond, A.I. (1994) Regulation of mammalian spliceosome assembly by a protein phosphorylation mechanism. *EMBO J.*, **13**, 5679–5688.
68. Maris, C., Dominguez, C. and Allain, F.H. (2005) The RNA recognition motif, a plastic RNA-binding platform to regulate post-transcriptional gene expression. *FEBS J.*, **272**, 2118–2131.
69. Petoukhov, M.V., Monie, T.P., Allain, F.H., Matthews, S., Curry, S. and Svergun, D.I. (2006) Conformation of polypyrimidine tract binding protein in solution. *Structure*, **14**, 1021–1027.
70. de la Mata, M. and Kornblihtt, A.R. (2006) RNA polymerase II C-terminal domain mediates regulation of alternative splicing by SRp20. *Nat. Struct. Mol. Biol.*, **13**, 973–980.
71. Ceulemans, H. and Bollen, M. (2004) Functional diversity of protein phosphatase-1, a cellular economizer and reset button. *Physiol. Rev.*, **84**, 1–39.
72. Glatz, D.C., Rujescu, D., Tang, Y., Berendt, F.J., Hartmann, A.M., Faltraco, F., Rosenberg, C., Hulette, C., Jellinger, K., Hampel, H. *et al.* (2006) The alternative splicing of tau exon 10 and its regulatory proteins CLK2 and TRA2-BETA1 changes in sporadic Alzheimer's disease. *J. Neurochem.*, **96**, 635–644.
73. Sanford, J.R., Gray, N.K., Beckmann, K. and Caceres, J.F. (2004) A novel role for shuttling SR proteins in mRNA translation. *Genes Dev.*, **18**, 755–768.
74. Swartz, J.E., Bor, Y.C., Misawa, Y., Rekosh, D. and Hammarskjold, M.L. (2007) The shuttling SR protein 9G8 plays a role in translation of unspliced mRNA containing a constitutive transport element. *J. Biol. Chem.*, **282**, 19844–19853.
75. Brichta, L., Hofmann, Y., Hahnen, E., Siebzehnrubl, F.A., Raschke, H., Blumcke, I., Eyupoglu, I.Y. and Wirth, B. (2003) Valproic acid increases the SMN2 protein level: a well-known drug as a potential therapy for spinal muscular atrophy. *Hum. Mol. Genet.*, **12**, 2481–2489.
76. Cartegni, L. and Krainer, A.R. (2003) Correction of disease-associated exon skipping by synthetic exon-specific activators. *Nat. Struct. Biol.*, **10**, 120–125.
77. Hartmann, A.M., Nayler, O., Schwaiger, F.W., Obermeier, A. and Stamm, S. (1999) The interaction and colocalization of Sam68 with the splicing-associated factor YT521-B in nuclear dots is regulated by the Src family kinase p59(fyn). *Mol. Biol. Cell*, **10**, 3909–3926.
78. Stamm, S., Casper, D., Hanson, V. and Helfman, D.M. (1999) Regulation of the neuron-specific exon of clathrin light chain B. *Mol. Brain Res.*, **64**, 108–118.

79. Lorson, C.L., Hahnen, E., Androphy, E.J. and Wirth, B. (1999) A single nucleotide in the SMN gene regulates splicing and is responsible for spinal muscular atrophy. *Proc. Natl Acad. Sci. USA*, **96**, 6307–6311.
80. Butchbach, M.E., Guo, H. and Lin, C.L. (2003) Methyl-beta-cyclodextrin but not retinoic acid reduces EAAT3-mediated glutamate uptake and increases GTRAP3-18 expression. *J. Neurochem.*, **84**, 891–894.
81. Young, P.J., Le, T.T., thi Man, N., Burghes, A.H. and Morris, G.E. (2000) The relationship between SMN, the spinal muscular atrophy protein, and nuclear coiled bodies in differentiated tissues and cultured cells. *Exp. Cell. Res.*, **256**, 365–374.
82. Monani, U.R., Sendtner, M., Coovert, D.D., Parsons, D.W., Andreassi, C., Le, T.T., Jablonka, S., Schrank, B., Rossol, W., Prior, T.W. *et al.* (2000) The human centromeric survival motor neuron gene (SMN2) rescues embryonic lethality in Smn(−/−) mice and results in a mouse with spinal muscular atrophy. *Hum. Mol. Genet.*, **9**, 333–339.
83. Wang, Y., Wang, J., Gao, L., Lafyatis, R., Stamm, S. and Andreadis, A. (2005) Tau exons 2 and 10, which are misregulated in neurodegenerative diseases, are partly regulated by silencers which bind a complex comprised of SRp30c and SRp55 that either recruits or antagonizes htra2beta 1. *J. Biol. Chem.*, 14230–14239.
84. Brown, S.A., Ripperger, J., Kadener, S., Fleury-Olela, F., Vilbois, F., Rosbash, M. and Schibler, U. (2005) PERIOD1-associated proteins modulate the negative limb of the mammalian circadian oscillator. *Science*, **308**, 693–696.
85. Dong, B., Horowitz, D.S., Kobayashi, R. and Krainer, A.R. (1993) Purification and cDNA cloning of HeLa cell p54nrb, a nuclear protein with two RNA recognition motifs and extensive homology to human splicing factor PSF and Drosophila NONA/BJ6. *Nucleic Acids Res.*, **21**, 4085–4092.
86. Clark, J., Lu, Y.J., Sidhar, S.K., Parker, C., Gill, S., Smedley, D., Hamoudi, R., Linehan, W.M., Shipley, J. and Cooper, C.S. (1997) Fusion of splicing factor genes PSF and NonO (p54nrb) to the TFE3 gene in papillary renal cell carcinoma. *Oncogene*, **15**, 2233–2239.
87. Mercher, T., Busson-Le Coniat, M., Khac, F.N., Ballerini, P., Mauchauffe, M., Bui, H., Pellegrino, B., Radford, I., Valensi, F., Mugneret, F. *et al.* (2002) Recurrence of OTT-MAL fusion in t(1;22) of infant AML-M7. *Genes Chromosomes Cancer*, **33**, 22–28.
88. Ma, Z., Morris, S.W., Valentine, V., Li, M., Herbrick, J.A., Cui, X., Bouman, D., Li, Y., Mehta, P.K., Nizetic, D. *et al.* (2001) Fusion of two novel genes, RBM15 and MKL1, in the t(1;22)(p13;q13) of acute megakaryoblastic leukemia. *Nat. Genet.*, **28**, 220–221.
89. Chan, R.C. and Black, D.L. (1997) The polypyrimidine tract binding protein binds upstream of neural cell-specific c-src exon N1 to repress the splicing of the intron downstream. *Mol. Cell. Biol.*, **17**, 4667–4676.
90. Markovtsov, V., Nikolic, J.M., Goldman, J.A., Turck, C.W., Chou, M.Y. and Black, D.L. (2000) Cooperative assembly of an hnRNP complex induced by a tissue-specific homolog of polypyrimidine tract binding protein. *Mol. Cell. Biol.*, **20**, 7463–7479.
91. Yamamoto, H., Tsukahara, K., Kanaoka, Y., Jinno, S. and Okayama, H. (1999) Isolation of a mammalian homologue of a fission yeast differentiation regulator. *Mol. Cell. Biol.*, **19**, 3829–3841.